NASA/TM-2003-212440

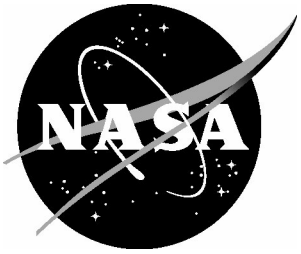

Hypervelocity Impact Test Results for a Metallic Thermal Protection System

Katherine L. Karr
The George Washington University,
Joint Institute for Advancement of Flight Sciences
Langley Research Center, Hampton, Virginia

Carl C. Poteet and Max L. Blosser,
Langley Research Center, Hampton, Virginia

August 2003

The NASA STI Program Office . . . in Profile

Since its founding, NASA has been dedicated to the advancement of aeronautics and space science. The NASA Scientific and Technical Information (STI) Program Office plays a key part in helping NASA maintain this important role.

The NASA STI Program Office is operated by Langley Research Center, the lead center for NASA's scientific and technical information. The NASA STI Program Office provides access to the NASA STI Database, the largest collection of aeronautical and space science STI in the world. The Program Office is also NASA's institutional mechanism for disseminating the results of its research and development activities. These results are published by NASA in the NASA STI Report Series, which includes the following report types:

- TECHNICAL PUBLICATION. Reports of completed research or a major significant phase of research that present the results of NASA programs and include extensive data or theoretical analysis. Includes compilations of significant scientific and technical data and information deemed to be of continuing reference value. NASA counterpart of peer-reviewed formal professional papers, but having less stringent limitations on manuscript length and extent of graphic presentations.

- TECHNICAL MEMORANDUM. Scientific and technical findings that are preliminary or of specialized interest, e.g., quick release reports, working papers, and bibliographies that contain minimal annotation. Does not contain extensive analysis.

- CONTRACTOR REPORT. Scientific and technical findings by NASA-sponsored contractors and grantees.

- CONFERENCE PUBLICATION. Collected papers from scientific and technical conferences, symposia, seminars, or other meetings sponsored or co-sponsored by NASA.

- SPECIAL PUBLICATION. Scientific, technical, or historical information from NASA programs, projects, and missions, often concerned with subjects having substantial public interest.

- TECHNICAL TRANSLATION. English-language translations of foreign scientific and technical material pertinent to NASA's mission.

Specialized services that complement the STI Program Office's diverse offerings include creating custom thesauri, building customized databases, organizing and publishing research results ... even providing videos.

For more information about the NASA STI Program Office, see the following:

- Access the NASA STI Program Home Page at ***http://www.sti.nasa.gov***

- E-mail your question via the Internet to help@sti.nasa.gov

- Fax your question to the NASA STI Help Desk at (301) 621-0134

- Phone the NASA STI Help Desk at (301) 621-0390

- Write to:
  NASA STI Help Desk
  NASA Center for AeroSpace Information
  7121 Standard Drive
  Hanover, MD 21076-1320

NASA/TM-2003-212440

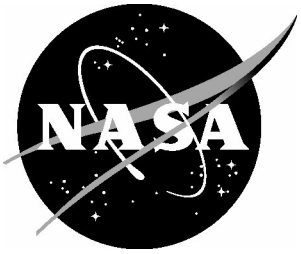

Hypervelocity Impact Test Results for a Metallic Thermal Protection System

Katherine L. Karr
The George Washington University,
Joint Institute for Advancement of Flight Sciences
Langley Research Center, Hampton, Virginia

Carl C. Poteet and Max L. Blosser,
Langley Research Center, Hampton, Virginia

National Aeronautics and
Space Administration

Langley Research Center
Hampton, Virginia 23681-2199

August 2003

Available from:

NASA Center for AeroSpace Information (CASI)
7121 Standard Drive
Hanover, MD 21076-1320
(301) 621-0390

National Technical Information Service (NTIS)
5285 Port Royal Road
Springfield, VA 22161-2171
(703) 605-6000

Abstract

Hypervelocity impact tests have been performed on specimens representing metallic thermal protection systems (TPS) developed at NASA Langley Research Center for use on next-generation reusable launch vehicles (RLV). The majority of the specimens tested consist of a foil gauge exterior honeycomb panel, composed of either Inconel 617 or Ti-6Al-4V, backed with 2.0 in. of fibrous insulation and a final Ti-6Al-4V foil layer. Other tested specimens include titanium multi-wall sandwich coupons as well as TPS using a second honeycomb sandwich in place of the foil backing. Hypervelocity impact tests were performed at the NASA Marshall Space Flight Center Orbital Debris Simulation Facility. An improved test fixture was designed and fabricated to hold specimens firmly in place during impact. Projectile diameter, honeycomb sandwich material, honeycomb sandwich facesheet thickness, and honeycomb core cell size were examined to determine the influence of TPS configuration on the level of protection provided to the substructure (crew cabin, fuel tank, etc.) against micrometeoroid or orbit debris impacts. Pictures and descriptions of the damage to each specimen are included.

Introduction

All vehicles subjected to the harsh environment of space are susceptible to impacts by micrometeoroids and orbital debris. Micrometeoroids and orbital debris are natural and man-made particles that travel in low earth orbit at velocities of up to 20 km/s. As man's activity in space increases so does the threat of hypervelocity impact.

There is an on-going effort at NASA Langley to develop a metallic thermal protection system (TPS) for the next-generation reusable launch vehicle (RLV). This next-generation RLV is intended to replace the US Space Shuttle for missions to low earth orbit. The TPS tiles, forming the exterior surface of the vehicle, must not only protect the RLV from aerodynamic heating during launch and re-entry but also protect the vehicle and crew from hypervelocity impacts during the mission. The metallic TPS is designed to be more durable and simpler to repair or replace than the current TPS tiles used on the Shuttle. The primary metallic TPS configuration studied herein is comprised of a metallic box encapsulating lightweight internal insulation. [1] The exterior surface of the box is either an Inconel 617 (will be referred to as Inconel) honeycomb sandwich or a Ti-6Al-4V (will be referred to as titanium) honeycomb sandwich. The inner surface is either a titanium honeycomb sandwich or a titanium foil layer, and the sides are made of either Inconel or titanium corrugated foil. The TPS panel configuration can be seen in Figure 1. In addition to the TPS configuration described above, titanium multiwall sandwich TPS was also studied. Titanium multiwall sandwich, as shown in Figure 2, consists of 9 alternating layers of flat and dimpled foil. [2,3]

To determine the effects of hypervelocity impacts on the metallic TPS concept, hypervelocity impact testing on various TPS configurations were performed at the NASA Marshall Space Flight Center Orbital Debris Simulation Facility. The effect on penetration of the substructure wall by varying the following parameters was examined: facesheet material, facesheet thickness, honeycomb core cell size, thickness of insulation, and projectile diameter.

The TPS parameter levels tested will be described in the “Test Specimens” section of this report. All tests were performed with an 1100-O Aluminum sphere of diameter 0.125 in., 0.1875 in., or 0.25 in. at velocities near 7 km/s. For each test the substructure wall, the simulated vehicle wall protected by the TPS, was a 10 in. x 10 in. specimen of Aluminum 2024-T81 of 0.1 in. thickness.

Background

In the past most hypervelocity impact testing has been performed to test shielding for spacecraft that will spend extended periods of time in space. Spacecraft that are designed for long duration exposure in Earth orbit typically use a Whipple shield [4,5], or a design derived from the Whipple Shield, to provide protection from space debris and micro-meteorites. Whipple determined that the ideal design for protecting against hypervelocity impacts consists of a thin sacrificial shield (or "bumper") separated by a standoff distance of several inches from the main shield. The purpose of the bumper is to break up the incident particle before it impacts the main shield. Impact between the particle and the bumper generates a shock wave that causes fragmentation, melting, and at high velocities, vaporization of the particle and portions of the bumper. It is interesting to note that the bumper does not have to be very thick relative to the particle diameter to be effective. Located several inches behind the bumper, the main shield is designed to absorb the resultant blast. Due to the ability of the bumper to spread out the damage over a wide area on the main shield, the required areal density of the bumper system is much less than a single wall system designed to defeat the same particle. [6] The standoff distance is very important in determining the effectiveness of a Whipple shield. Increasing the standoff gives the debris from the particle-bumper impact more time to spread out, increasing the protection. Figure 3 diagrams the result of a hypervelocity impact with a shield consisting of two bumper shields before the main shield, commonly known as a double-bumper shield.

Whipple shields are impractical for thermal protection systems. However, most of the TPS configurations examined have at least 2.0 in. of spacing between the exterior surface and the substructure and could act in a manner similar to the Whipple shield concept. In this case, the TPS panel will act as a bumper and the substructure takes the place of the main shield. Therefore, there is the potential that TPS can be effectively used to protect spacecraft from hypervelocity impacts.

Testing Facility

The impact test series was conducted at the Orbital Debris Simulation Facility at NASA Marshall Space Flight Center in Huntsville, Alabama. The facility houses a two stage light gas gun that is used for meteoroid/space debris impact simulations. The light gas gun can accommodate 2.5 mm (0.098 in.) to 12.7 mm (0.5 in.) diameter spherical projectiles and up to 1.6 mm (0.063 in.) diameter cylindrical projectiles. Projectile mass ranges from 0.0004 to 2.1 grams and travel at velocities from 2 to 7.5 km/s. There are three test chambers of the following sizes:

1. 0.4 m (16 in.) x 0.4 m (16 in.) x 0.4 m (16 in.)
2. 0.66 m (26 in.) x 0.66 m (26 in.) x 1.2 m (48 in.)
3. 2.4 m (8 ft) diameter x 6.1 m (20 ft) long

Also available, are real time in situ diagnostics such as velocity measurements, debris cloud momentum measurement and 24 channel simultaneous high speed analog to digital data recording. Velocity measurements are taken using flash X-ray, Hall (Streak) camera, and ultra high-speed cameras. The gun can be fired a maximum of three times per day with a pointing error of approximately one inch square. [7]

It can be seen in Figure 4 that the light gas gun consists of the following sections: the breech, the pump tube, the high-pressure section, and the launch tube. The breech has an 8.89 cm (3.5 in.) inner diameter and is 60.96 cm (2 ft) in length. It is designed to withstand 50,000 psi internal pressure, however, during routine testing the pressure is kept lower than 20,000 psi. The pump tube has a 6.35 cm (2.5 in.) inner diameter and is 3.048 m (10 ft) long. The pump tube contains pressurized hydrogen in front of a polyethylene piston used to compress the gas. The high-pressure section is tapered from the pump tube to the 12.7 mm (0.5 in.) diameter barrel. A metal diaphragm burst disc separates the high-pressure section from the barrel. The barrel has a 12.7 mm (0.5 in.) inner diameter and is 2.59 m (102 in.) long. The high-pressure gases produced in the high-pressure section also have very high temperatures. This high

temperature gas can erode the barrel wall as it flows down the barrel behind the projectile. This is the main reason hydrogen is used in the light gas gun instead of helium. Due to the basic difference in molecular weight and in the ratio of specific heats, hydrogen gas operates at one-fifth the temperature of helium gas for equivalent performance. [8]

Operation of the light gas gun occurs as follows. The propellant is ignited by application of electrical current to an explosive squib. The piston is then released when the pressure generated by the burning propellant reaches a predetermined value. The propellant accelerates the piston from 550 m/sec (1800 ft/sec) to 915 m/sec (3000 ft/sec). The hydrogen gas, loaded into the pump tube before firing, is compressed by the advancing piston. At a predetermined pressure value, the metal burst disc opens in a petaling fashion along grooves accurately machined on the disc surface. The projectile, placed approximately two inches in front of the burst disc, is accelerated by the released gas. For best results, a constant pressure on the base of the projectile would be ideal. However, the pressure behind the projectile has a tendency to drop as the projectile accelerates. To compensate for this normal decrease, the pressure in the high-pressure section must be continuously increased. This is accomplished with a taper in the high-pressure section. As the piston protrudes into the taper, the volume of gas gets smaller. Therefore, a fixed amount of forward movement of the piston is very effective in raising the pressure. The taper has been designed to increase the pressure fast enough to compensate for the decrease in pressure due to expansion into the barrel.

Test Hardware

The test hardware consisted of two items: the fixture to hold the specimens in place during testing and the specimens themselves. This section will detail how these two items were designed and fabricated.

Hypervelocity Test Fixture

The original test fixture available at Marshall Space Flight Center for the hypervelocity testing consisted of a vise that provided a clamping force along a two-inch span on the bottom edge of the specimen. In previously performed tests, it has been suggested that when the specimen is supported in this manner, unwanted vibrations can occur. It was found that when the projectile impacts the specimen a pressure wave ahead of the remaining projectile particles causes the top portion of the specimen to vibrate while the bottom portion remains relatively stationary in the vise. To control this vibration, a fixture was designed that can support, on all four sides, a variety of differently sized specimens and configurations. The front and side views of this fixture are depicted in Figures 5 and 6. Figure 7 shows the full test setup with specimens in place. Figure 8 shows a detailed view of the spacer plate and a specimen comprised of an outer honeycomb panel, insulation, and inner honeycomb panel.

The fixture contains many now standardized features. On August 23, 1995 a meeting was held in Downey, California to discuss, among other items, the standardization of hypervelocity testing for TPS. Participants in this meeting included representatives from Rockwell, NASA Marshall, NASA Langley, and NASA Ames. It was determined that the following items would be standard requirements for all hypervelocity tests conducted on TPS systems:

- Test Sample Size - 6 in. x 6 in. TPS for impact particles less than or equal to 0.25 inches
- Test Sample Fixture - Entire test fixture must be stiff. Four-sided clamping is required, 0.75 in. around edge of specimen. Knife-edge clamping is acceptable, but not required.
- Substructure - 0.1 in. Al 2024-T851 of size 10 in. x 10 in. (This represents one orbiter substructure; if determined to be suitable, an alternative temper may be acceptable, such as -T3, or -T81)
- Witness Plate - 0.25 in. minimum thickness of Al 2024-T3. Locate 3.0 in. behind the substructure
- Angle - When number of test is limited, angle of impact should be 0˚, normal to the test sample.
- Impact Velocity - When limited to a single velocity, use 8 km/sec (for a maximum of 0.25 in. spherical projectile).
- Projectile - 1100-O Aluminum spheres

All of the above requirements were taken into consideration when designing and fabricating the impact fixture. [9]

The fixture was designed to be versatile in order to accommodate many different types of TPS in different sizes and configurations. The test fixture, as shown in Figure 5, can be adapted to fit various specimen sizes by replacing the front plate. The front plate is very simple to manufacture so that a variety of different size specimens could be tested with very little manufacturing costs. Two front plates were fabricated for these tests, one for 4 in. x 4 in. specimen and one for 6 in. x 6 in. specimen. The fixture also contains a spacer plate. This spacer allows the experimenter to have a second layer of material spaced away from the substructure, where the substructure represents the spacecraft wall that is being protected. TPS spacing from the substructure may be different for different configurations of TPS and, therefore, it is important to provide a means to accommodate this variable. The spacer plate is also equipped with knife-edge supports on the back side to simply support the substructure. The knife-edges are a separate piece and can be easily replaced with flat fillers if the experimenter does not feel it is necessary to have the substructure simply supported. The back plate, as labeled in Figure 6, is the main support of the entire fixture and contains the other side of the knife-edge supports. The back plate holds the 10 in. x 10 in. substructure in place and the knife-edges, as on the spacer plate, are detachable. The knife-edges on both the spacer and the

back plate are offset 0.75 in. from the specimen edges as specified above. As can be seen in the figure, the back plate has stiff vertical supports that will help to dampen out any vibrations that may occur. The final plate on the fixture is the witness plate holder. The holder is design to hold the 10 in. x 10 in. witness plate in a range of distances from the substructure, but was kept at 3.0 in. in these tests as specified by the standardization.

Test Specimens

The test specimens for this test series were built up from layers of Inconel and titanium honeycomb sandwich materials, titanium multi-wall, fibrous insulation, and titanium foil. Table I contains a description of the different types of honeycomb sandwich materials used. The first column lists a material ID that will be used to identify honeycomb core configurations throughout this paper. The first number in the ID represents the facesheet gauge, in mils, the second component is the honeycomb material, where "Inc hc" stands for Inconel honeycomb and "Ti hc" stands for titanium honeycomb, and the final component is the honeycomb cell size, in inches.

All Inconel honeycomb specimens except for "5.0 Inc hc 3/16" specimens were fabricated by B. F. Goodrich (previously Rohr Industries) as part of a previous effort. Both "3.0 Ti hc 3/16" and "14.0 Ti hc 3/16" specimens were also fabricated in a previous effort. The other listed honeycomb specimens were made by B. F. Goodrich specifically for this test series, using similar manufacturing techniques. These techniques, as well as the techniques used to make the titanium multiwall specimens, are briefly described in the following paragraphs.

Table I. Honeycomb Sandwich Materials

Material ID	Material	Facesheet Gauge (in)	Core Gauge (in)	Core Depth (in)	Cell Size (in)
2.5 Inc hc 1/4	Inconel	0.0025	0.002	0.28	0.25
5.0 Inc hc 1/4	Inconel	0.005	0.002	0.28	0.25
5.0 Inc hc 3/16	Inconel	0.005	0.0015	0.28	0.1875
10.0 Inc hc 1/4	Inconel	0.01	0.002	0.28	0.25
3.0 Ti hc 3/16	Titanium	0.003	0.0015	0.17	0.1875
5.0 Ti hc 3/16	Titanium	0.005	0.0015	0.28	0.1875
14.0 Ti hc 3/16	Titanium	0.014	0.0015	0.17	0.1875

To fabricate the Inconel honeycomb sandwiches, the square-cell honeycomb core was fabricated from 0.002 in. or 0.0015 in. thick corrugated foil ribbons. The depth of the core was 0.28 inches. A braze alloy (1.97B-0.02C-13.13Cr-3.4Fe-Ni balance) was applied to one side of each facesheet. The honeycomb core was placed between the facesheets adjacent to the braze and the assembly was placed on a flat reference surface in a vacuum furnace. Tungsten pellets were placed on the assembly to provide contact pressure for the diffusion brazing process. The furnace was evacuated to 10^{-4} torr and heated to 2150 ˚F. The assembly was held at this temperature for 3 minutes, cooled to 1900 ˚F, and then held at this temperature for 1 hour.

The titanium honeycomb sandwich core was manufactured from 0.0015 in. thick corrugated foil ribbons. After being cleaned, the edges of the honeycomb core were plated with an alloy to promote Liquid Interface Diffusion (LID). [10] A more detailed description of the fabrication procedure for the Inconel and titanium sandwich panels can be found in Reference [7].

The titanium multi-wall specimens were a nine-sheet sandwich structure consisting of an upper and lower facesheet, four dimpled sheets, and three septum sheets. The thicknesses of the sheets were 0.004, 0.003, 0.003, and 0.0015 in. for the upper facesheet, lower facesheet, dimpled sheets, and septum sheets, respectively, before processing. The Liquid Interface Diffusion (LID) bonding system was used by Rohr to join the dimpled sheets to the flat sheets.

The dimpled sheets were superplastically formed, using the same process parameters reported in References [2,3]. The skins and septum sheets were square sheared, and then process cleaned. The dimpled sheets were plated on each node and when put in contact with each other and heated to approximately 1214˚ K (1725˚ F), the plating material melts creating a short time eutectic with the titanium. While holding at this temperature for a specified time the plating material is completely diffused into the titanium creating a bond at all plated interfaces. [1] The finished titanium multi-wall sandwich thickness was 0.68 inches.

Saffil™ fibrous insulation was used to represent the TPS insulation layer. Saffil is an alumina-based fiber that can be used at temperatures in excess of 2900 °F. In general, 2.0 in. of insulation was used. However, several tests varied the insulation thickness from 1.5 in. to 3.0 in. Ti-multiwall TPS did not use fibrous insulation. The density of Saffil varies depending on how tightly it is packed into the TPS panel. Unfortunately, the insulation weight was not measured prior to testing, however subsequent weight measurements of likely packing densities suggest that the Saffil density was between 7.35 E-4 and 9.5 E-4 lb/in^3.

Many metallic TPS configurations make use of a titanium foil on the back of the fibrous insulation layer. In this work, a 0.003 in. titanium foil was used, and will be referred to as "3.0 Ti foil".

All of the sandwich specimens used in this testing were cut into their respective sizes from the larger fabricated pieces at the LaRC machine shop using a wet diamond saw. Table II is the test matrix describing how the different types of materials were combined to make a TPS specimen. Table II will be discussed in detail in the next section.

Test Procedure

A test matrix was developed to efficiently use the available honeycomb sandwich material to characterize the response of metallic TPS to hypervelocity impact. Table II is the

test matrix that was used in this test series. The first column is the test number and the second column is the size of the specimen. The third, fourth and fifth columns describe the outer-panel of the specimen, the insulation thickness and the inner-panel of the specimen respectively, where the ids defined in Table I are used to identify honeycomb sandwich configurations. The sixth and seventh columns describe the projectile diameter and impact velocity. Finally, the last column is the specimen weight, which is the combined weight of the outer-panel and the inner-panel, but does not include insulation or substructure weight. For several specimens the weight was not determined. The dependent variables in the test series were measures of damage to the specimen, to be described subsequently.

All tests were performed with an 1100-O aluminum sphere near 7 km/sec. The projectile diameters used were 0.125 in., 0.187 in., and 0.25 inches. The substructure for each test was 0.1 in. thick 2024-T81 aluminum plates of 10 in. x 10 in. size and the witness plate was a 10 in. x 10 in. 2024-T3 aluminum plate 0.25 in. thick. As shown in Figure 8, all tests were performed with a 0.09” spacing between the back face of the inner-panel, or outer-panel in the case of titanium multiwall specimens, and the front face of the substructure.

Test numbers 1-9 will give insight into how changing the thickness of the Inconel facesheet will effect penetration and hole size parameters. The same honeycomb cell size was used while varying outer-panel facesheet gauge and projectile diameter. Test numbers 3 and 5 resulted in bad shots that did not yield usable data. To replace shot number 5, specimen number 6 was shot with the 0.187 in. diameter projectile instead of the 0.25 in. diameter projectile as originally planned.

Test numbers 10-12 were conducted to determine the effect of honeycomb cell size on substructure damage. The test parameters are identical to tests 4 and 6, however the outer-panel honeycomb cell size is changed from 0.25 in. to 0.1875 in.

Test numbers 13-21 used titanium honeycomb sandwiches as the outer-panel instead of Inconel. The three titanium honeycomb sandwich configurations defined in Table I were impacted with a range of projectile diameters. Test number 13 resulted in a bad shot that did not provide useful results. This test was repeated in test 15 with a 0.125 in. diameter projectile but the projectile velocity was not determined.

Tests 22-24 were performed incorrectly and will not be described further. Tests 25-27 maintained a constant facesheet thickness of Inconel honeycomb in the outer panel and used titanium honeycomb with varying facesheet thicknesses as the inner panel. The same projectile was used in these three tests. Shot numbers 28-30 were performed on titanium multi-wall samples with varied diameter projectiles. Finally tests 31-33 were performed to replace tests 22-24. The purpose of these tests was to determine the influence of insulation thickness on substructure damage.

Table II. Hypervelocity Test Matrix

Hypervelocity Impact Test Matrix 1100-O Al Projectile 2024-T81 0.1" Substruture							
Specimen Number	**Specimen Size**	**Outer Panel**	**Ins. Thick (in)**	**Inner Panel**	**Proj. Dia. (in)**	**Proj. Vel. (km/s)**	**Specimen Weight (g)**
1	4 in. x 4 in.	2.5 Inc hc 1/4	2.0	3.0 Ti foil	0.125	7.5	28
2	6 in. x 6 in.	2.5 Inc hc 1/4	2.0	3.0 Ti foil	0.187	7.4	60
3	6 in. x 6 in.	2.5 Inc hc 1/4	2.0	3.0 Ti foil	0.25	Bad Shot	62
4	4 in. x 4 in.	5.0 Inc hc 1/4	2.0	3.0 Ti foil	0.125	7.3	30
5	6 in. x 6 in.	5.0 Inc hc 1/4	2.0	3.0 Ti foil	0.187	Bad Shot	79
6	6 in. x 6 in.	5.0 Inc hc 1/4	2.0	3.0 Ti foil	0.187	7.5	80
7	4 in. x 4 in.	10.0 Inc hc 1/4	2.0	3.0 Ti foil	0.125	7.6	60
8	6 in. x 6 in.	10.0 Inc hc 1/4	2.0	3.0 Ti foil	0.187	7.9	125
9	6 in. x 6 in.	10.0 Inc hc 1/4	2.0	3.0 Ti foil	0.25	7.2	120
10	4 in. x 4 in.	5.0 Inc hc 3/16	2.0	3.0 Ti foil	0.125	7.3	30
11	6 in. x 6 in.	5.0 Inc hc 3/16	2.0	3.0 Ti foil	0.187	7.4	88
12	6 in. x 6 in.	5.0 Inc hc 3/16	2.0	3.0 Ti foil	0.25	7.4	85
13	4 in. x 4 in.	3.0 Ti hc 3/16	2.0	3.0 Ti foil	0.125	Bad Shot	?
14	6 in. x 6 in.	3.0 Ti hc 3/16	2.0	3.0 Ti foil	0.187	7.5	24
15	6 in. x 6 in.	3.0 Ti hc 3/16	2.0	3.0 Ti foil	0.125	?	28
16	4 in. x 4 in.	5.0 Ti hc 3/16	2.0	3.0 Ti foil	0.125	7.6	?
17	6 in. x 6 in.	5.0 Ti hc 3/16	2.0	3.0 Ti foil	0.187	7.1	40
18	6 in. x 6 in.	5.0 Ti hc 3/16	2.0	3.0 Ti foil	0.25	7.4	38
19	4 in. x 4 in.	14.0 Ti hc 3/16	2.0	3.0 Ti foil	0.125	7.8	40
20	6 in. x 6 in.	14.0 Ti hc 3/16	2.0	3.0 Ti foil	0.187	7.6	68
21	6 in. x 6 in.	14.0 Ti hc 3/16	2.0	3.0 Ti foil	0.25	7.6	65
22	4 in. x 4 in.	5.0 Inc hc 1/4	1.5	3.0 Ti foil	0.125	Bad Test	30
23	4 in. x 4 in.	5.0 Inc hc 1/4	2.5	3.0 Ti foil	0.125	Bad Test	35
24	4 in. x 4 in.	5.0 Inc hc 1/4	3.0	3.0 Ti foil	0.125	Bad Test	31
25	4 in. x 4 in.	5.0 Inc hc 3/16	2.0	3.0 Ti hc 3/16	0.125	?	50
26	4 in. x 4 in.	5.0 Inc hc 3/16	2.0	5.0 Ti hc 3/16	0.125	7.0	51
27	4 in. x 4 in.	5.0 Inc hc 3/16	2.0	14.0 Ti hc 3/16	0.125	7.1	68
28	4 in. x 4 in.	Ti Multiwall	n/a	n/a	0.125	7.0	30
29	4 in. x 4 in.	Ti Multiwall	n/a	n/a	0.187	7.1	31
30	4 in. x 4 in.	Ti Multiwall	n/a	n/a	0.25	?	29
31	4 in. x 4 in.	5.0 Inc hc 3/16	1.5	3.0 Ti foil	0.125	7	?
32	4 in. x 4 in.	5.0 Inc hc 3/16	2.5	3.0 Ti foil	0.125	Bad Shot	?
33	4 in. x 4 in.	5.0 Inc hc 3/16	3.0	3.0 Ti foil	0.125	7.1	?

Results

The NASA Marshall facility successfully completed 26 of the 33 hypervelocity tests planned for this test series. The description of the damage and photos of the specimens are provided in Appendix A. The top portion of each page contains the test number and a description of the projectile diameter, projectile velocity, and the specimen. The top rows of photos are the front faces of the outer panel, inner panel and substructure with the description of the damage printed below the photo. The insulation is not pictured because in most cases it was torn into many pieces and a hole size could not be determined. The second rows of photos are the back faces of the outer panel, inner panel and substructure specimens with a damage description printed below the photo. As can be seen from the photos and the descriptions, except for test 27, all projectiles penetrated through the outer panel and inner panel with significant amounts of damage. Sandwich panel holes were larger on the back surface than on the front surface due to the debris cloud expanding during penetration.

Three methods were used to examine the impacted specimens: Penetration / no penetration, substructure hole area, and substructure damage characteristics. The key findings using each method will be described. The following discussion section will explain the significance of these findings.

Penetration / No Penetration

Table III lists substructure penetration results for the various TPS configurations tested. The honeycomb ids defined in Table I are used to specify outer-panel and inner-panel parameters. The "Total Areal Density" reported is based on experimental measurements excluding the aluminum substructure, and is explained in the subsequent section. The average value of Total Areal Density is reported for rows containing multiple specimens. Under the

"Projectile Diameter" heading, penetration results are listed for the three projectile diameters tested. The symbol "X" is used to denote no penetration, "O" to represent penetration, and "-" to represent an untested projectile size. Penetration is defined herein as a visible hole. Examining specimens 1 through 12, it can be seen that all specimens with an Inconel outer-panel were capable of stopping 1/8 in. projectiles. Penetration occurred with all tests using 3/16 in. or ¼ in. projectile sizes. It is impossible to determine the influence of Inconel outer-panel facesheet gauge or cell size on the level of protection provided to the substructure based solely on the available penetration / no penetration data.

Table III. Substructure Penetration Data

(X: No penetration, O: Penetration, -: Untested)

Specimen Numbers	TPS Configuration				Projectile Diameter		
	Outer Panel	Insulation Thickness (in)	Inner Panel	Total Areal Density (lb/in^2)	1/8 in.	3/16 in.	1/4 in.
1,2	2.5 Inc hc 1/4	2.0	3.0 Ti foil	0.0057	X	O	-
4,6	5.0 Inc hc 1/4	2.0	3.0 Ti foil	0.0064	X	O	-
7-9	10.0 Inc hc 1/4	2.0	3.0 Ti foil	0.0097	X	O	O
10-12	5.0 Inc hc 3/16	2.0	3.0 Ti foil	0.0068	X	O	O
14,15	3.0 Ti hc 3/16	2.0	3.0 Ti foil	0.0035	O	O	-
16-18	5.0 Ti hc 3/16	2.0	3.0 Ti foil	0.0043	O	O	O
19-21	14.0 Ti hc 3/16	2.0	3.0 Ti foil	0.0065	X	O	O
25	5.0 Inc hc 3/16	2.0	3.0 Ti hc 3/16	0.0088	X	-	-
26	5.0 Inc hc 3/16	2.0	5.0 Ti hc 3/16	0.0089	X	-	-
27	5.0 Inc hc 3/16	2.0	14.0 Ti hc 3/16	0.0113	X	-	-
28-30	Ti Multiwall	n/a	n/a	0.0041	X	O	O
31	5.0 Inc hc 3/16	1.5	3.0 Ti foil	0.0056	X	-	-
33	5.0 Inc hc 3/16	3.0	3.0 Ti foil	0.007	X	-	-

Tests 14 through 21 used titanium outer-panels in place of Inconel. The 1/8 in. projectiles penetrated the substructure of all specimens except the "14.0 Ti hc 3/16" outer-panel TPS, and all larger diameter projectiles resulted in substructure penetration. Based on this data, it is clear that the "14.0 Ti hc 3/16" outer-panel TPS offers improved protection compared to the thinner gauge titanium honeycomb sandwich outer-panel TPS. Comparing Inconel and titanium

honeycomb sandwich outer-panel TPS with similar facesheet gauges, such as “2.5 Inc hc ¼” panels to “3.0 Ti hc 3/16” panels or “5.0 Inc hc ¼” and “5.0 Inc hc 3/16” panels to “5.0 Ti hc 3/16” panels” it can be seen that for a given facesheet thickness Inconel honeycomb sandwich outer-panel TPS provides better protection than titanium honeycomb sandwich outer-panel TPS. However, the titanium TPS is significantly lighter. From the available penetration / no penetration data it is impossible to determine whether the titanium or Inconel TPS provide better protection to the substructure at comparable total areal densities.

In the tests described thus far, the TPS configuration consisted of an outer honeycomb sandwich panel, an insulation layer, and an inner titanium foil layer. Tests 25 through 27 used titanium honeycomb sandwich panels in place of the inner titanium foil layer. The outer-panel consisted of “5.0 Inc hc 3/16” panels. The facesheet gauge of the inner-panel was increased in each successive test. All tests in this series were conducted with 1/8 in. projectiles, none of which resulted in substructure penetration. There was no significant substructure surface damage in any of these tests, and the “14.0 Ti hc 3/16” inner-panel contained the impact debris without penetration of the inner facesheet.

Tests 28 through 30 tested the titanium multiwall TPS. The multiwall TPS contained no fibrous insulation layer or inner-panel, and the spacing between the inner surface of the titanium multiwall and the substructure was only 0.09 inches. Substructure penetration did not occur for the 1/8 in. projectile, but all larger particles resulted in penetration. Comparing the titanium multiwall TPS penetration data to titanium honeycomb sandwich outer-panel TPS penetration data of similar weight (“5.0 Ti hc 3/16”), it is clear that the multiwall TPS provides better protection to the substructure. This is surprising considering the fact that the titanium multiwall TPS has a considerably smaller standoff (0.77 in.) than the “5.0 Ti hc 3/16” TPS (2.37 in.), which limits the amount of time for the debris cloud to expand prior to substructure impact.

However, titanium multiwall is not as efficient as an insulator, resulting in significantly heavier TPS designs for most RLV reentry vehicle trajectories of interest. [11]

Finally, tests 31 through 33 were used to determine the influence of varying the insulation layer thickness. The same configuration of outer and inner-panels was used as in tests 10 through 12, however the thickness of insulation was varied between 1.5 and 3.0 inches. Tests were performed with 1/8 in. particles, none of which resulted in substructure penetration.

Examination of penetration data was useful in determining the range of projectile sizes over which different TPS configurations were capable of protecting the substructure. Presenting this in tabular format, as in Table III is also useful for identifying where future testing would be beneficial. In tests with Inconel honeycomb sandwich outer-panels (tests 1 through 12) testing with projectile diameters in between 1/8 in. and 3/16 in. would be useful in determining the influence of outer-panel facesheet thickness and honeycomb cell size on substructure penetration. With the lighter weight titanium outer-panels (tests 14 through 21) testing with projectile diameters under 1/8 in. would be useful for the "3.0 Ti hc 3/16" and "5.0 Ti hc 3/16" outer-panel TPS configurations, and testing with projectile diameters between 1/8 in. and 3/16 in. would be useful for the "14.0 Ti hc 3/16" outer-panel TPS configuration. It would be very useful to test with projectile diameters larger than 1/8 in. using the TPS configurations from tests 25 through 27 and 31 through 33.

Substructure Hole Area

To gain a better understanding of the influence of various TPS parameters in protecting the substructure, it was decided to examine the substructure hole area versus the areal density of the various TPS specimens. Table IV shows the calculation of TPS specimen nominal weights, excluding braze weight. In these calculations, honeycomb was assumed to be 1.6% the density of the bulk material. Unfortunately, no measurements were made of the insulation weight used

in the experiments. A subsequent measurement revealed an estimated density range between 7.35E-4 and 9.5E-4 lb/in^3. For this reason an upper bound and lower bound are listed in Table IV. Substructure weight is not included in the calculation of areal density.

Specimen weights without insulation were measured prior to testing, and are reported in Table II. These were used, along with the estimated insulation density to calculate the measured areal density for each specimen. The measured areal densities are compared with the calculated areal densities in Table V. "Structural areal density" refers to the TPS specimen without insulation. "Total areal density, lower bound" refers to areal density calculated using the lower bound estimate for insulation density, and "total areal density, upper bound" refers to areal density calculated using the upper bound estimate for insulation density. Weight measurements were not obtained for several specimens. For these specimens, weights were estimated based on other specimens with similar configurations. There is a surprising variation of measured areal densities for specimens that are nominally the same. For example, structural areal densities for specimens 10 through 12 and 19 through 21 vary by 32% and 38%, respectively. This degree of variation is surprisingly large for specimens cut from the same panel, and is not fully understood. The degree of variation for other specimens is smaller. In the discussion to follow, the measured "total areal density, upper bound" will be used since it should represent a good estimate of the actual specimen areal density. Using calculated or lower bound values was found to lead to the same interpretation of the results.

To quantify the amount of substructure damage, the area of the hole formed in the aluminum substructure, or the combined area when multiple holes were present, was used as a damage parameter. The last column in Table V reports the measured substructure hole areas for the TPS specimens tested.

Table IV. Calculation of TPS Areal Density

(Units: lb/in^2)

	Outer Panel			**Insulation**		**Inner Panel**			**TOTAL**		
Specimen Number	Outer Facesheet	H/C	Inner Facesheet	Lower Bound	Upper Bound	Outer Facesheet	H/C	Inner Facesheet	Structural	Structural + Insulation, Lower Bound	Structural + Insulation, Upper Bound
1	0.00076	0.00135	0.00076	0.00147	0.00190	0.00048	0.00000	0.00000	0.00334	0.0048	0.0052
2	0.00076	0.00135	0.00076	0.00147	0.00190	0.00048	0.00000	0.00000	0.00334	0.0048	0.0052
3	0.00076	0.00135	0.00076	0.00147	0.00190	0.00048	0.00000	0.00000	0.00334	0.0048	0.0052
4	0.00151	0.00135	0.00151	0.00147	0.00190	0.00048	0.00000	0.00000	0.00485	0.0063	0.0067
5	0.00151	0.00135	0.00151	0.00147	0.00190	0.00048	0.00000	0.00000	0.00485	0.0063	0.0067
6	0.00151	0.00135	0.00151	0.00147	0.00190	0.00048	0.00000	0.00000	0.00485	0.0063	0.0067
7	0.00302	0.00135	0.00302	0.00147	0.00190	0.00048	0.00000	0.00000	0.00787	0.0093	0.0098
8	0.00302	0.00135	0.00302	0.00147	0.00190	0.00048	0.00000	0.00000	0.00787	0.0093	0.0098
9	0.00302	0.00135	0.00302	0.00147	0.00190	0.00048	0.00000	0.00000	0.00787	0.0093	0.0098
10	0.00151	0.00135	0.00151	0.00147	0.00190	0.00048	0.00000	0.00000	0.00485	0.0063	0.0067
11	0.00151	0.00135	0.00151	0.00147	0.00190	0.00048	0.00000	0.00000	0.00485	0.0063	0.0067
12	0.00151	0.00135	0.00151	0.00147	0.00190	0.00048	0.00000	0.00000	0.00485	0.0063	0.0067
13	0.00048	0.00044	0.00048	0.00147	0.00190	0.00048	0.00000	0.00000	0.00188	0.0033	0.0038
14	0.00048	0.00044	0.00048	0.00147	0.00190	0.00048	0.00000	0.00000	0.00188	0.0033	0.0038
15	0.00048	0.00044	0.00048	0.00147	0.00190	0.00048	0.00000	0.00000	0.00188	0.0033	0.0038
16	0.00080	0.00072	0.00080	0.00147	0.00190	0.00048	0.00000	0.00000	0.00280	0.0043	0.0047
17	0.00080	0.00072	0.00080	0.00147	0.00190	0.00048	0.00000	0.00000	0.00280	0.0043	0.0047
18	0.00080	0.00072	0.00080	0.00147	0.00190	0.00048	0.00000	0.00000	0.00280	0.0043	0.0047
19	0.00224	0.00044	0.00224	0.00147	0.00190	0.00048	0.00000	0.00000	0.00540	0.0069	0.0073
20	0.00224	0.00044	0.00224	0.00147	0.00190	0.00048	0.00000	0.00000	0.00540	0.0069	0.0073
21	0.00224	0.00044	0.00224	0.00147	0.00190	0.00048	0.00000	0.00000	0.00540	0.0069	0.0073
25	0.00151	0.00135	0.00151	0.00147	0.00190	0.00048	0.00044	0.00048	0.00577	0.0072	0.0077
26	0.00151	0.00135	0.00151	0.00147	0.00190	0.00080	0.00072	0.00080	0.00669	0.0082	0.0086
27	0.00151	0.00135	0.00151	0.00147	0.00190	0.00224	0.00044	0.00224	0.00929	0.0108	0.0112
31	0.00151	0.00135	0.00151	0.00110	0.00143	0.00048	0.00000	0.00000	0.00485	0.0060	0.0063
32	0.00151	0.00135	0.00151	0.00184	0.00238	0.00048	0.00000	0.00000	0.00485	0.0067	0.0072
33	0.00151	0.00135	0.00151	0.00221	0.00285	0.00048	0.00000	0.00000	0.00485	0.0071	0.0077

Table V. Comparison of Substructure Hole Area vs. Calculated and Measured TPS Areal Density

Specimen Number	Test Parameters				Calculated			Measured			Results
	Outer Panel	Insulation Thickness (in)	Inner Panel	Projectile Diameter (in)	Structural Areal Density (lb/in^2)	Total Areal Density, Lower Bound (lb/in^2)	Total Areal Density, Upper Bound (lb/in^2)	Structural Areal Density (lb/in^2)	Total Areal Density, Lower Bound (lb/in^2)	Total Areal Density, Upper Bound (lb/in^2)	Substructure Hole Area (in^2)
1	2.5 Inc hc 1/4	2.0	3.0 Ti foil	0.125	0.0033	0.0048	0.0052	0.0039	0.0053	0.0058	0
2	2.5 Inc hc 1/4	2.0	3.0 Ti foil	0.188	0.0033	0.0048	0.0052	0.0037	0.0051	0.0056	0.028
4	5.0 Inc hc 1/4	2.0	3.0 Ti foil	0.125	0.0048	0.0063	0.0067	0.0041	0.0056	0.0060	0
6	5.0 Inc hc 1/4	2.0	3.0 Ti foil	0.188	0.0048	0.0063	0.0067	0.0049	0.0064	0.0068	0.0007
7	10.0 Inc hc 1/4	2.0	3.0 Ti foil	0.125	0.0079	0.0093	0.0098	0.0083	0.0097	0.0102	0
8	10.0 Inc hc 1/4	2.0	3.0 Ti foil	0.188	0.0079	0.0093	0.0098	0.0077	0.0091	0.0096	0.00023
9	10.0 Inc hc 1/4	2.0	3.0 Ti foil	0.250	0.0079	0.0093	0.0098	0.0073	0.0088	0.0092	0.435
10	5.0 Inc hc 3/16	2.0	3.0 Ti foil	0.125	0.0048	0.0063	0.0067	0.0041	0.0056	0.0060	0
11	5.0 Inc hc 3/16	2.0	3.0 Ti foil	0.188	0.0048	0.0063	0.0067	0.0054	0.0069	0.0073	0.00196
12	5.0 Inc hc 3/16	2.0	3.0 Ti foil	0.250	0.0048	0.0063	0.0067	0.0052	0.0067	0.0071	0.51
14	3.0 Ti hc 3/16	2.0	3.0 Ti foil	0.188	0.0019	0.0033	0.0038	0.0015	0.0029	0.0034	0.14
15	3.0 Ti hc 3/16	2.0	3.0 Ti foil	0.125	0.0019	0.0033	0.0038	0.0017	0.0032	0.0036	0.0037
16	5.0 Ti hc 3/16	2.0	3.0 Ti foil	0.125	0.0028	0.0043	0.0047	0.0024	0.0039	0.0043	0.0017
17	5.0 Ti hc 3/16	2.0	3.0 Ti foil	0.188	0.0028	0.0043	0.0047	0.0024	0.0039	0.0043	0.066
18	5.0 Ti hc 3/16	2.0	3.0 Ti foil	0.250	0.0028	0.0043	0.0047	0.0023	0.0038	0.0042	1.75
19	14.0 Ti hc 3/16	2.0	3.0 Ti foil	0.125	0.0054	0.0069	0.0073	0.0055	0.0070	0.0074	0
20	14.0 Ti hc 3/16	2.0	3.0 Ti foil	0.188	0.0054	0.0069	0.0073	0.0042	0.0056	0.0061	0.00023
21	14.0 Ti hc 3/16	2.0	3.0 Ti foil	0.250	0.0054	0.0069	0.0073	0.0040	0.0055	0.0059	1.66
25	5.0 Inc hc 3/16	2.0	3.0 Ti hc 3/16	0.125	0.0058	0.0072	0.0077	0.0069	0.0084	0.0088	0
26	5.0 Inc hc 3/16	2.0	5.0 Ti hc 3/16	0.125	0.0067	0.0082	0.0086	0.0070	0.0085	0.0089	0
27	5.0 Inc hc 3/16	2.0	14.0 Ti hc 3/16	0.125	0.0093	0.0108	0.0112	0.0094	0.0108	0.0113	0
28	Ti Multiwall	n/a	n/a	0.125	0.0041	0.0041	0.0041	0.0041	0.0041	0.0041	0
29	Ti Multiwall	n/a	n/a	0.188	0.0041	0.0041	0.0041	0.0043	0.0043	0.0043	0.0133
30	Ti Multiwall	n/a	n/a	0.250	0.0041	0.0041	0.0041	0.0040	0.0040	0.0040	0.75
31	5.0 Inc hc 3/16	1.5	3.0 Ti foil	0.125	0.0048	0.0060	0.0063	0.0041	0.0052	0.0056	0
33	5.0 Inc hc 3/16	3.0	3.0 Ti foil	0.125	0.0048	0.0071	0.0077	0.0041	0.0063	0.0070	0

The substructure hole area is plotted versus the measured "total areal density, upper bound" for four configurations of TPS specimen in Figure 9. The test series are "Inc hc 3/16" outer-panels (tests 1-9, circles), "Inc hc 3/16" outer-panels (tests 10-12, boxes), "Ti hc 3/16" outer-panels (tests 14-21, diamonds), and titanium multiwall outer-panels (tests 28-30, X's). Note that in Figure 9 only the outer-panel is specified, but that areal density for the entire TPS specimen, consisting of an outer-panel, insulation, and inner-panel, is implied. For simplicity, this convention will be used throughout the remaining discussion. In Figure 9, circles, boxes, diamonds, and X's denote the four configurations, respectively. These symbols are used consistently in the figures to follow. Symbol size is varied to represent the size of the projectile, with the smallest symbol used to represent 1/8 in. projectiles and the largest symbol used to represent ¼ in. projectiles. Examination of Figure 9 reveals that ¼ in. projectiles produced significantly larger holes in the substructure than the smaller projectiles tested. Hole areas for ¼ in. projectiles range from on the order of 0.5 in^2 for TPS specimens using Inconel outer-panels to 1.75 in^2 for specimens using titanium honeycomb sandwich outer-panels. Although both "Ti hc 3/16" outer-panel TPS specimens tested were lower areal density than the "Inc hc ¼" and "Inc hc 3/16" outer-panel TPS specimens, it appears likely that for equivalent areal density TPS, using Inconel honeycomb sandwich outer-panels in place of titanium honeycomb sandwich outer-panels will reduce the substructure hole size. Impact of the "Ti multiwall" TPS specimen with a ¼ in. projectile produced a 0.75 in^2 substructure hole area, significantly lower than the hole area for the comparable areal density "5.0 Ti hc 3/16" outer-panel TPS specimen. It is unclear from the data how the "Ti multiwall" TPS compares to the "Inc hc 1/4" and "Inc hc 3/16" outer-panel TPS when impacted with ¼ in. projectiles, since there is no test data at comparable areal densities.

Figure 10 focuses on the 3/16 in. projectile impacts and expands the scale used for substructure hole area in the previous figure. Note that all 3/16 in. projectiles resulted in

substructure penetration (Table III), however due to the wide range of substructure hole size several of the hole areas listed in Figure 10 appear to be no penetration when they are actually pin-hole sized penetrations. For 3/16 in. projectiles, the substructure hole size did not appear to be significantly influenced by variation of the honeycomb cell size between "Inc hc ¼" and "Inc hc 3/16" outer-panels. Comparison of data from "Ti hc 3/16" and "Inc hc ¼" outer-panel TPS configurations reveal that the material of the outer-panel does not significantly influence results with 3/16 in. projectiles near the limit of substructure zero hole size. Finally, impact of the "Ti Multiwall" specimen generated smaller substructure holes than impact of the "Ti hc 3/16" outer-panel specimen of comparable areal density, and it is reasonable to hypothesize that tests for an "Inc hc ¼" outer-panel specimen of comparable areal density would result in larger hole sizes than the "Ti Multiwall" specimen.

Figure 11 shows the substructure hole area of TPS specimens impacted with 1/8 in. particles, further expanding the scale for substructure hole area from the previous slides. Impact of "3.0 Ti hc 3/16" and "5.0 Ti hc 3/16" outer-panel specimens resulted in substructure penetration. All other impacts with 1/8 in. particles resulted in no penetration. Note that the trend line drawn for "Ti hc 3/16" outer-panel specimens can be misleading, since it implies that penetration occurs for this TPS configuration at areal densities under 0.0074 lb/in^2 when in fact penetration is likely to occur somewhere between 0.0043 and 0.0074 lb/in^2. Therefore, a comparison between "Inc hc ¼" and "Ti hc 3/16" outer-panel specimens can not be made, since it is not clear what the largest areal density is, for either configuration, that allows penetration of the substructure. However, a comparison can be made between the "Ti Multiwall" specimen and the "Ti hc 3/16" specimen. At comparable areal densities, the "Ti hc 3/16" outer-panel specimen allows substructure penetration, where the "Ti Multiwall" specimen does not.

Substructure Damage Characteristics

In addition to the measurement of hole areas, the substructure damage was examined qualitatively to gain an understanding of the damage mechanisms present. Table VI is a summary of the qualitative damage characteristics that were discernable in each test. Most tests resulted in a varying degree of cratering on the surface of the substructure, due to solid fragments in the impact debris. Fragment holes were created when solid fragments with enough energy to penetrate individually, or by multiple impacts in the same area, denoted "Fragment Impact Overlap" in Table VI, were present.

Substructure bulging resulted mainly in tests with ¼ in. projectiles, however impact with a 3/16 in. projectile on a TPS specimen using an "5.0 Ti hc 3/16" outer layer also produced a visible substructure bulge. Substructure bulging resulted from extensive transfer of momentum from the impact debris to the substructure, resulting in deformation of the substructure. In all cases where this phenomenon was observed, penetration of the substructure resulted. It is interesting to note that the only test with a ¼ in. projectile that did not result in substructure bulging was the test performed on the "Ti Multiwall" specimen. Substructure tearing was observed in all tests where substructure bulging occurred except in test number 17, which used a 3/16 in. projectile. The longest substructure tear was observed in specimen 21, and was 1.1 in. in length.

Normal impacts on typical Whipple shields tend to produce symmetrical debris clouds. However, several impact tests with TPS specimens produced distinct damage zones in the substructure. It is hypothesized that this is due to the honeycomb layer splitting the debris cloud flow when the projectile impact zone is oriented over a cell wall or cell wall junction. The distinct damage zones may also be due to breakup of the projectile prior to impact with the specimen, a phenomena common in hypervelocity impact testing.

A 0.2 x 0.05 in. titanium foil fragment was found adhered to the surface of the aluminum substructure in test 1. Since test 1 used an Inconel outer-panel, the titanium fragment was a part of the inner-panel that was propelled by the impact debris toward the substructure. As was mentioned earlier, evidence of cratering due to solid fragments was also found on many specimens. Many tests also left molten deposits on the substructure. Taking this data together it is clear that the impact debris consisted of small solid fragments, molten debris, and in some cases lower velocity fragments from the TPS. In addition, a blue or purple discoloring was noticed on most of the substructure surfaces. It is possible that this was due to exposure to hot gases in the impact debris, or perhaps oxidation after testing.

In addition to the characteristics noted above, black deposits covered portions of the substructure in many tests. These deposits were formed from remaining particles of the sabot or explosive squib that were not deflected. Adequate deflection of the sabot was a problem with many of the tests performed, and in some cases resulted in damage to the TPS and possibly the substructure.

Table VI. Substructure Damage Characteristics

Specimen Number	Cratering	Fragment Holes	Fragment Impact Overlap	Substructure Bulge	Substructure Tearing	Distinct Damage Zones	Solid Foil Fragment	Molten Deposit	Blue/ Purple Discoloring
1							Yes	Yes	Yes
2	Yes	Yes	Yes			Yes			Yes
4	Yes					Yes		Yes	Yes
6	Yes	Yes	Yes					Yes	Yes
7	Yes		Yes						Yes
8	Yes	Yes	Yes					Yes	
9	Yes	Yes	Yes	Yes	Yes	Yes			
10	Yes		Yes			Yes			Yes
11	Yes	Yes							Yes
12	Yes	Yes	Yes	Yes	Yes			Yes	Yes
14	Yes	Yes	Yes			Yes		Yes	
15		Yes	Yes			Yes			Yes
16	Yes	Yes	Yes			Yes			Yes
17	Yes	Yes	Yes	Yes					
18				Yes	Yes			Yes	Yes
19	Yes								Yes
20		Yes						Yes	Yes
21	Yes	Yes	Yes	Yes	Yes			Yes	Yes
25								Yes	
26									Yes
27									
28	Yes							Yes	
29	Yes	Yes	Yes					Yes	Yes
30	Yes	Yes	Yes					Yes	Yes
31								Yes	
33	Yes	Yes							

Discussion

The findings reported in the previous section, when taken together, give some insight into the effect of various TPS parameters on the degree of hypervelocity impact protection provided to the substructure. This section will discuss the effect of using titanium versus Inconel honeycomb sandwich outer-panel TPS, the influence of outer-panel facesheet gauge, the effect of outer-panel honeycomb cell size, and the impact behavior of Ti multiwall TPS versus the honeycomb outer-panel TPS. In addition, the limitations of using substructure hole size as a damage parameter will be discussed.

Comparison of Inconel and titanium TPS

Based on penetration of the substructure (Table III), it was seen that for a given honeycomb sandwich outer-panel facesheet gauge Inconel panels provided better protection to the substructure than titanium panels. This result is to be expected, since Inconel is denser than titanium. However, most aerospace designs will be weight driven. If instead the substructure hole areas are compared versus TPS areal density (Table V), it is not clear which material provides the best substructure impact protection. Tests with 3/16 in. projectiles result in similar substructure hole sizes. Tests with 1/8 in. projectiles were inconclusive. Interestingly, tests with ¼ in. projectiles produced larger substructure holes in the titanium TPS specimens than they did in Inconel TPS specimens of similar areal density. It is not clear why the hole sizes were equivalent for 3/16 in. projectiles and different for ¼ in. projectiles. This may be due to mechanisms occurring during the ¼ in. impacts that are not present in the 3/16 in. impacts, such as an increased interaction with the honeycomb or a different projectile breakup behavior due to the different wall thickness to projectile diameter ratio. However, the impact process is highly nonlinear, and with the limited data available these hypotheses should be considered speculation.

At this point, it should also be noted that the use of substructure hole size as an indicator of the impact shield effectiveness could be misleading. The rationale for this argument is shown graphically in Figure 12, where conceptual drawings of three different impact cases are shown. The first case, labeled "No Bumper" represents impact on an unprotected structure. The "Thin Bumper" case represents impact with a bumper / substructure system where the bumper is too thin to provide adequate protection, and the "Thick Bumper" case represents a shielding system that successfully protects against the impact. As can be seen, since the "No Bumper" case does not disperse the projectile prior to substructure impact, a smaller hole is created than in the "Thin Bumper" case. However, the "No Bumper" case represents a higher energy impact to the substructure. In the final case, the "Thick Bumper", the projectile is dispersed enough to prevent substructure penetration. Surface damage and possibly deformation of the substructure are likely, but substructure penetration is prevented.

Applying this example to the ¼ in. projectile impacts it is not clear whether Inconel or titanium TPS offers better protection. Although, for comparable areal densities, substructure hole size is smaller for Inconel TPS than titanium TPS, this information can not be used to conclude that the Inconel TPS is more effective than titanium TPS. If the reasoning in Figure 12 is followed, the larger substructure hole size in titanium TPS tests may indicate that the titanium TPS is actually dispersing the projectile to a greater extent than Inconel TPS of similar areal density, and is therefore a more effective protection. However, this hypothesis cannot be substantiated based on the data available.

Effect of Outer-panel Facesheet Gauge

The thickness of the outer-panel facesheets had a large influence on the substructure hole size when 1/8 in. and 3/16 in. particles were used. Tests with the ¼ in. projectile did not appear to be as sensitive to the facesheet gauge. Increasing the facesheet gauge from 0.005 in.

to 0.014 in. in tests with titanium honeycomb outer-panels reduced the substructure hole size by only 5%. Increasing the facesheet gauge from 0.005 to 0.010 in. in tests with Inconel honeycomb outer-panels (and switching from 3/16 in. cell size to ¼ in. cell size) reduced the substructure hole size by 15%. Phenomenologically the holes were similar, consisting of bulging and tearing of the substructure.

Effect of Honeycomb Cell Size

For the range of TPS parameters and projectile sizes tested, variation of the cell size had no appreciable effect on substructure penetration or hole size. It is thought that the influence of the honeycomb will be largely dependent on the impact location relative to the honeycomb core, where the results could be substantially different depending on whether impact occurred in the middle of a cell or over a ribbon. The effect of honeycomb, and honeycomb cell size, is therefore anticipated to be highly random. For this reason, it is felt that multiple tests should be performed for each combination of TPS configuration and projectile size. If there is significant variation between test results with all the test parameters fixed, the source of the variation is likely to be due to the honeycomb. Several tests produced distinct damage zones on the substructure. It is possible that this was due to the honeycomb, which indicates that the honeycomb is influencing the formation of the debris cloud. However, the distinct damage zones could also be due to premature projectile break-up prior to impact with the TPS specimen.

Titanium Multiwall Specimens

Based on the penetration data in Table III, it can be seen that the titanium multiwall TPS resulted in better impact protection against 1/8 in. projectiles than TPS specimens of comparable areal density that used titanium honeycomb sandwich outer-panels. The

substructure hole sizes generated when testing titanium multiwall TPS with the three projectile diameters considered was equal to or smaller than titanium or Inconel honeycomb sandwich TPS of comparable areal density. (Figures 9, 10, 11) However, as was noted earlier, the hole size measurement can be misleading. Comparing the substruture damage characteristics of the ¼ in. projectile test of the titanium multiwall specimen to the honeycomb TPS specimens tested with the same projectile size reveals that, while the honeycomb TPS specimens experienced substructure bulging and tearing, impact of the titanium multiwall specimen produced a large substructure hole without bulging or tearing. It is hypothesized that this represents a higher energy impact of the substructure in the titanium multiwall test, resulting in a clean hole instead of significant structural deformation. If this hypothesis is correct, the titanium multiwall TPS is less effective at disrupting the ¼ in. particles than the other TPS configurations tested. However, it should be noted that the standoff distance (distance from outer surface to substructure) was 0.77 in. for titanium multiwall specimens and was between 2.26 and 2.54 in. for the other TPS specimens studied. Standoff distance is one of the most important parameters in determining impact protection, with increases in distance greatly increasing protection. It is possible that if the titanium multiwall specimens were tested at the same standoff distance as the other TPS specimens that the impact protection provided would be significantly increased.

Conclusions

This paper reports the results from a series of 33 hypervelocity impact tests performed on various metallic TPS configurations. The purpose of these tests was to determine the degree of protection provided to the substructure against hypervelocity impact. Taken as a whole, all but the lowest areal density TPS configurations were capable of preventing substructure penetration by 1/8 in. projectiles. All specimens that were tested with 3/16 in. projectiles were penetrated, however the substructure hole area changed significantly depending on the TPS areal density and configuration. In all tests performed with ¼ in. projectiles a large hole was produced in the substructure. The holes produced by ¼ in. projectile impacts were not only larger than those produced by the smaller projectiles, but they were qualitatively different, with most ¼ in. projectile tests producing significant substructure bulging and tearing.

It is unclear whether, for a given areal density, titanium or Inconel honeycomb sandwich TPS offers better protection to the substructure. The penetration data available is inconclusive. All tests with the 3/16 in. projectile resulted in penetration. Although two of the titanium honeycomb outer-panel TPS specimens were penetrated by 1/8 in. projectiles, the specimen areal density was significantly lower than the lowest areal density Inconel honeycomb sandwich TPS tested. Substructure hole size was identified as a second measure of the degree of impact protection. Use of substructure hole size was inconclusive for 1/8 in. particles. For 3/16 in. particles, similar substructure hole sizes were produced for Inconel and titanium honeycomb sandwich outer-panel TPS of comparable areal density. However, for ¼ in. projectiles the resulting substructure hole size was larger for titanium honeycomb sandwich outer-panel TPS than for Inconel honeycomb sandwich outer-panel TPS of comparable areal density. It is possible that a new mechanism becomes dominant in the ¼ in. projectile impacts, resulting in different impact behavior.

Although substructure hole size is useful in determining the extent of damage to the substructure, it may be misleading if used to determine the impact protection provided by different TPS configurations. The rationale behind this argument is that a poorly disrupted projectile may produce a small hole in a given substructure. A slightly improved shielding design will increase the dispersion of the projectile, but if this dispersion is still inadequate a larger substructure hole will be generated. Finally, an adequate shielding design will disperse the impact to the extent that the substructure is capable of resisting penetration.

Applying this argument to the ¼ in. projectile impacts described above, it can only be concluded that the Inconel honeycomb sandwich outer-panel TPS reduced the damage to the substructure. The degree of dispersion and kinetic energy of the impact debris cannot be determined from the test data, so the shielding effectiveness of the various TPS configurations cannot be determined.

The effect of honeycomb, and honeycomb cell size, on impact protection could not be determined from substructure penetration or hole size data. However, examination of the characteristics of substructure damage revealed distinct damage zones in several tests. It is possible that these distinct damage zones are the result of the honeycomb redirecting impact debris flow. However, it is also possible that the distinct damage zones resulted from projectile break up or damage prior to impact with the TPS specimen.

Titanium multiwall TPS prevented 1/8 in. projectiles from penetrating the substructure, while titanium honeycomb TPS of equivalent areal density allowed penetration. In addition, for comparable areal densities and for all particle sizes studied, tests with titanium multiwall produced smaller substructure hole sizes than tests with titanium honeycomb sandwich outer-panel TPS. However, qualitative examination of the substructure damage resulting from ¼ in. projectile impact reveals a large hole without significant structural deformation in the test with titanium multiwall but significant substructure bulging and tearing in all other tests with the ¼

in. particle. It is possible that this is due to the impact debris being more concentrated in the test with titanium multiwall, resulting in a clean hole instead of substructure bulging. This conclusion is supported by the fact that the standoff distance in titanium multiwall TPS was roughly 33% of the distance used in honeycomb TPS, reducing the time the impact debris had to disperse.

Although the test data obtained should be beneficial in the future design of metallic TPS to withstand the orbital debris environment, several areas were identified where further testing would be useful. Penetration data is very useful in determining the shielding effectiveness of the TPS. However, to draw conclusions for many of the parameters investigated, further testing is required over a wider range of particle sizes. In addition, it is anticipated that honeycomb core will have a variable effect on the projectile, depending on the impact location relative to the honeycomb core. To better understand the effect of honeycomb core, multiple tests could be conducted at a fixed particle size and TPS configuration. It is possible that variation in the results will give an estimate of the honeycomb core effect on impact protection. In addition, it would be useful to take flash x-ray radiographs in future tests, so that impact debris dispersion can be determined. Other techniques to determine the dispersion and velocity of the debris cloud could also be investigated.

8.0 References:

1. Anderson, J., LeHolm, R. B., Meaney, J. E., Rosenthal, H. A., "Development of Reusable Metallic Thermal Protection System Panels for Entry Vehicles," NASA-CR-181783, August 1989.

2. Blair, Winford, Meaney, John E., Jr., Rosenthal, Herman A., "Design and Fabrication of Titanium Multi-Wall Thermal Protection System (TPS) Test Panels," NASA CR- 159241, February, 1980.

3. Blair, Winford, Meaney, J. E., Jr., Rosenthal, H. A., "Fabrication of Titanium Multi-Wall Thermal Protection System (TPS) Test Panel Arrays," NASA CR-159383, December, 1980.

4. Whipple, F. L., White, C. S., Benson, O. O., "Meteoroid Phenomena and Meteorites, Physics and Medicine of the Upper Atmosphere," University of New Mexico Press, Albuquerque, NM 1952.

5. Whipple, F. L., "Meteorites and Space Travel," Astronomical Journal, No. 1161, 1947, p. 131.

6. Elfer, N. and Kovacevic, G., "Design for Space Debris Protection," 3rd Annual AIAA Greater New Orleans Section Symposium, November 7-8, 1985.

7. Tayler, Ray A., "A Space Debris Simulation Facility for Spacecraft Materials Evaluation," SAMPE Quarterly, Vol. 18, No 2, January 1987, pp. 28-34.

8. Nolen, Angela M., Zwiener, J. M., "Hypervelocity Impact Facility Building 4612," NASA MFSC.

9. Robinson, Jennifer, "Trip Report, Rockwell Metallic Thermal Protection System Meeting," Personal Communication Letter, August 31, 1995.

10. Gorton, Mark P., Shideler, John L., Web, Granville L., "Static and Aerothermal Tests of a Superalloy Honeycomb Prepackaged Thermal Protection System," NASA Technical Paper 3257, March 1993.

11. Myers, D. E., Martin, C. J., Blosser, M. L., "Parametric Weight Comparison of Advanced Metallic, Ceramic Tile, and Ceramic Blanket Thermal Protection Systems," NASA/TM-2000-210289, June 2000.

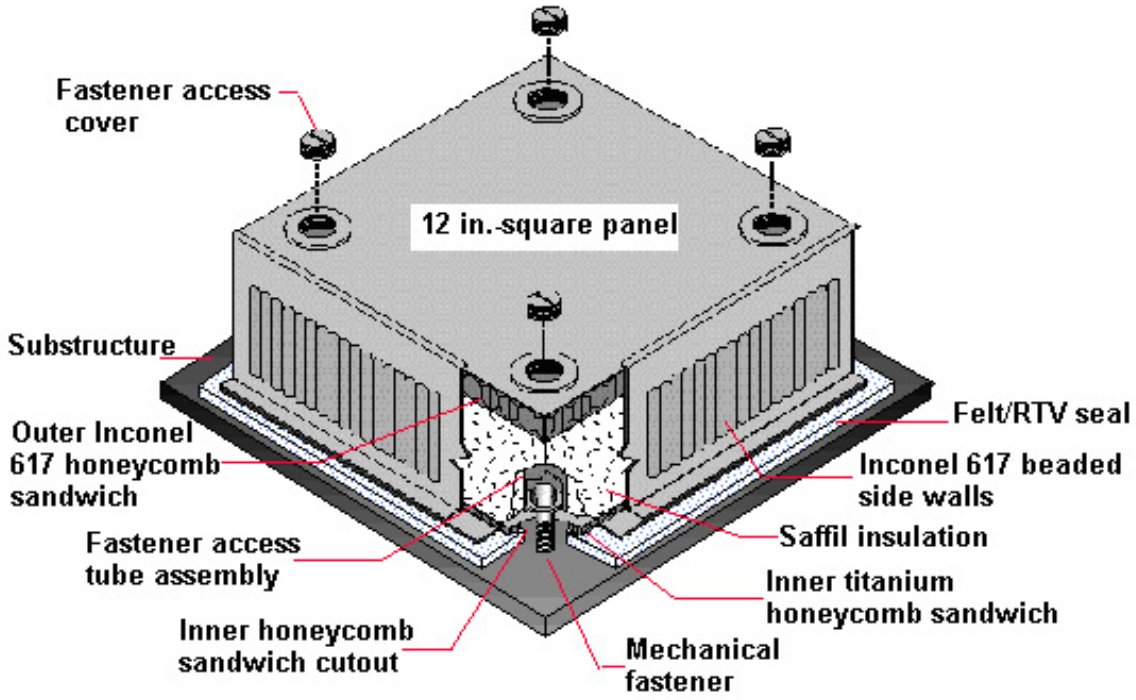

Figure 1: Metallic TPS Panel Configuration

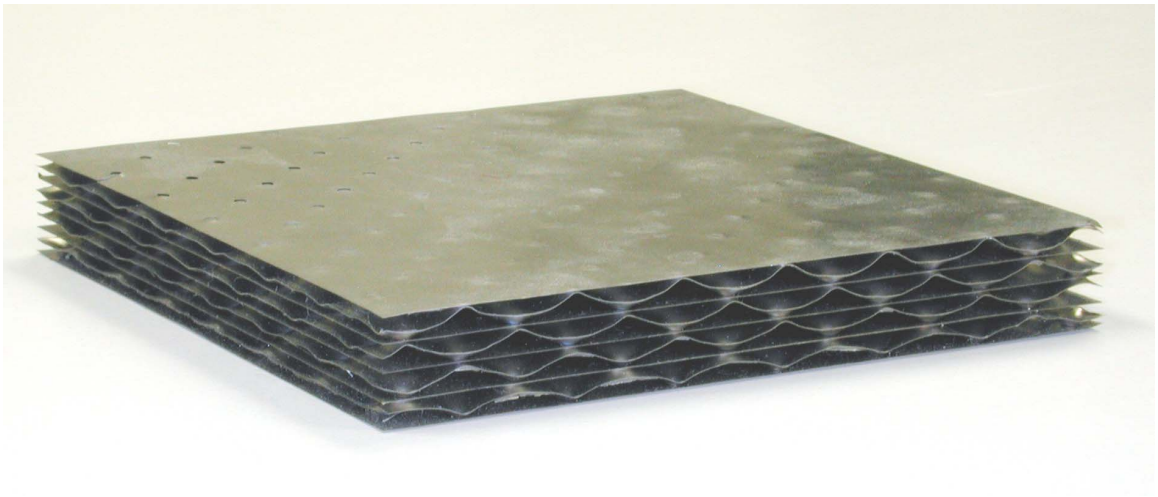

Figure 2. Titanium Multiwall TPS

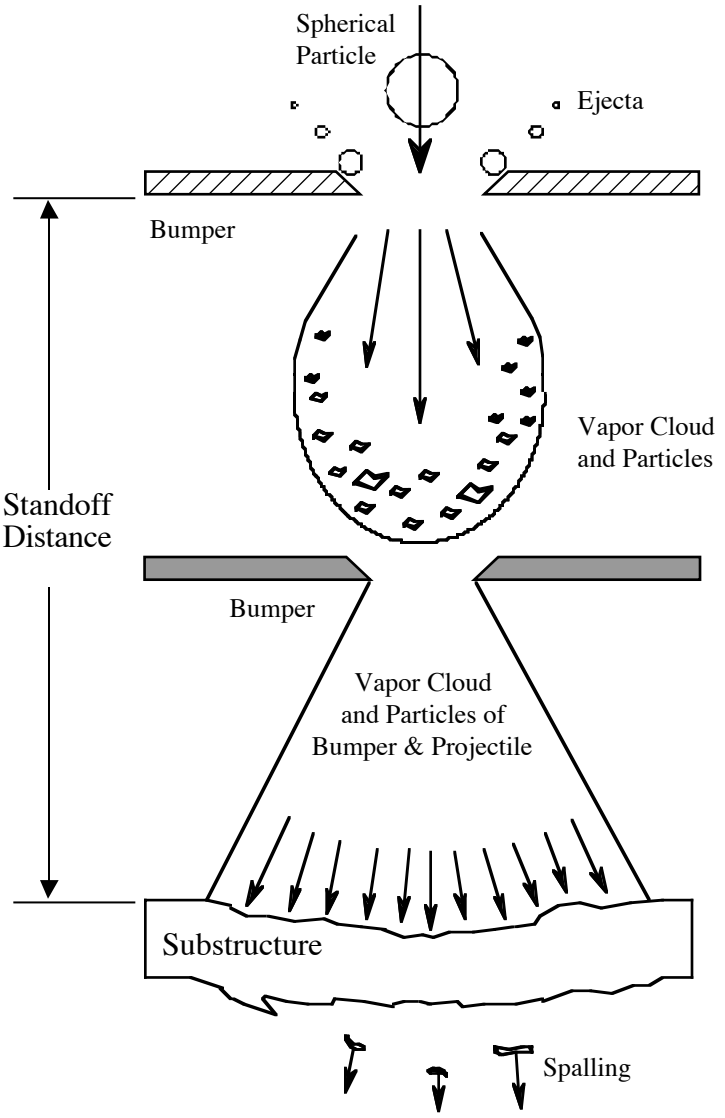

Figure 3: Schematic representation of a hypervelocity impact of a spherical particle with a multiple layer target.

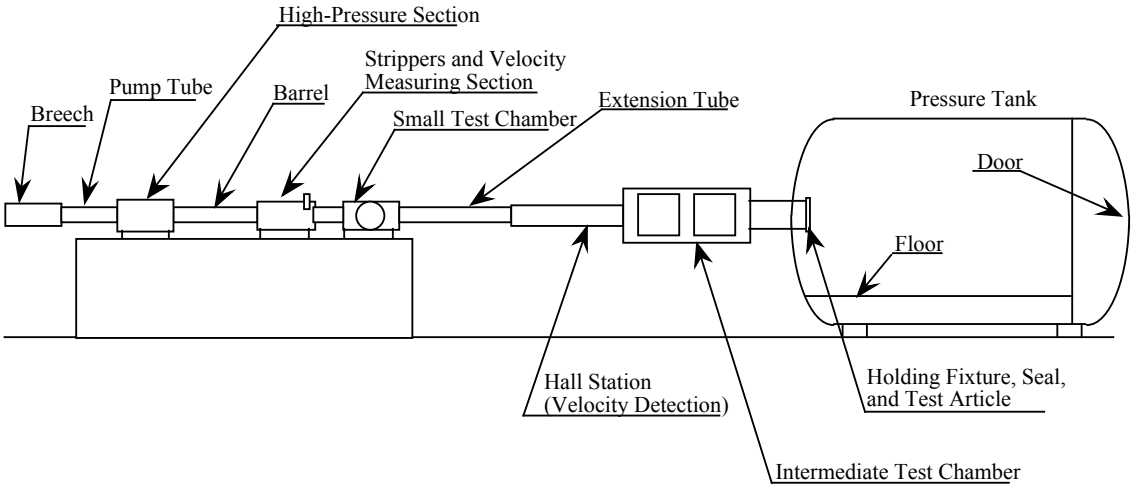

Figure 4: Schematic representation of Marshall Space Flight Center Light Gas Gun

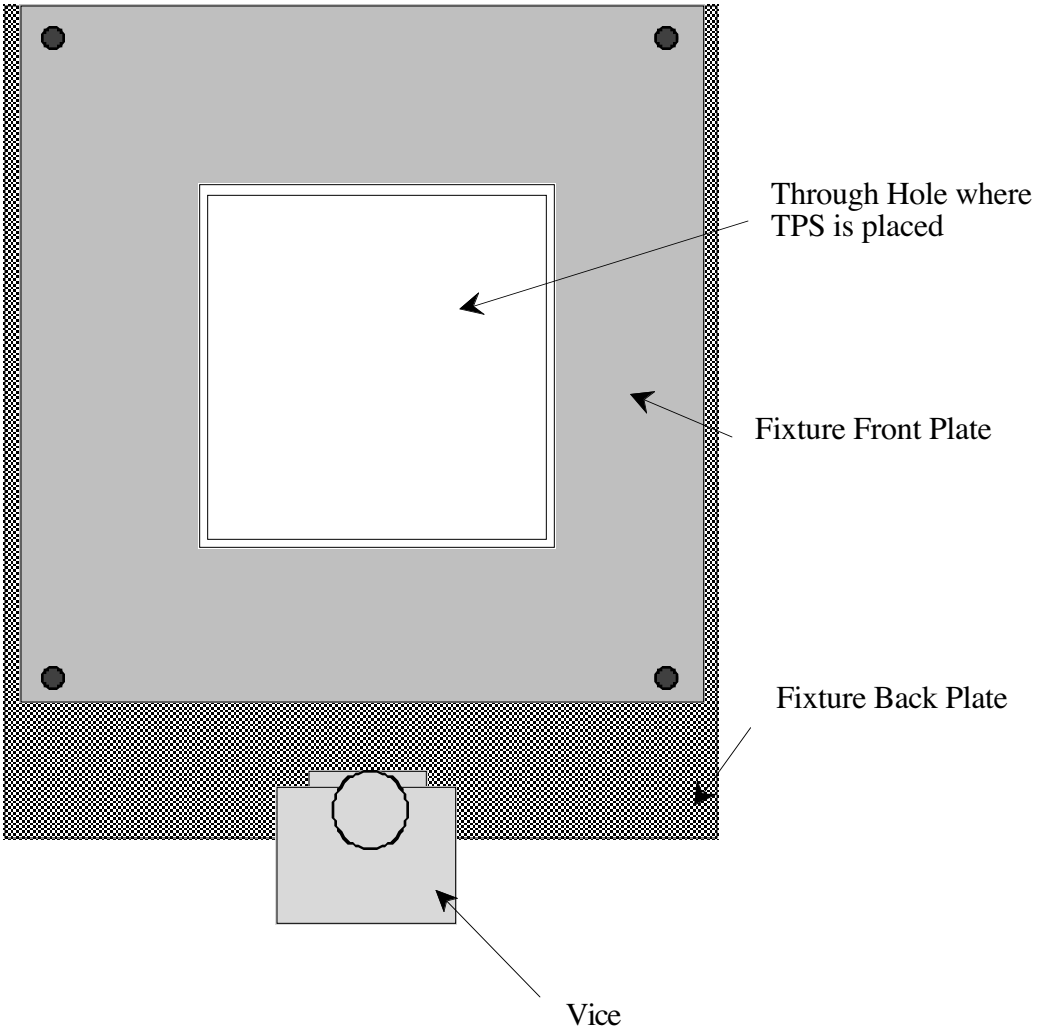

Figure 5: Front schematic view of hypervelocity impact test specimen holder.

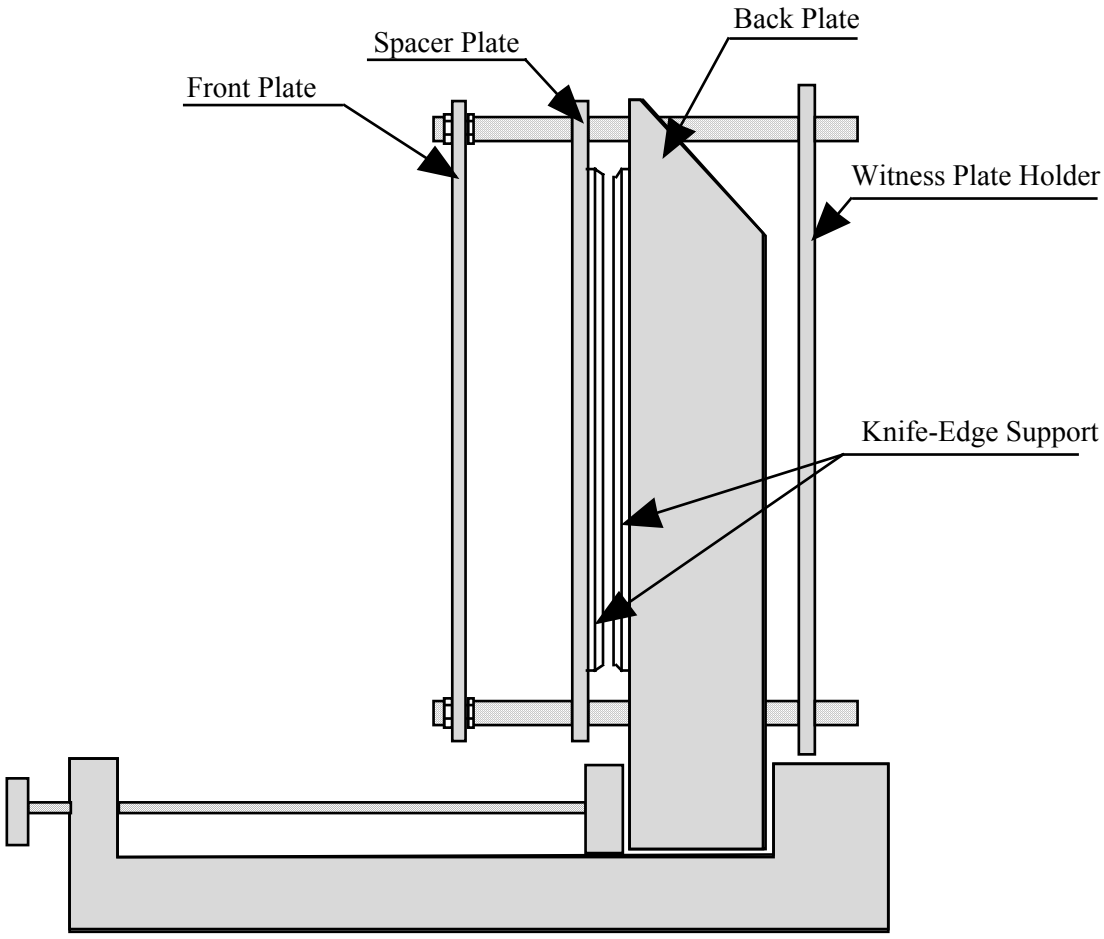

Figure 6: Side schematic view of hypervelocity impact test specimen holder.

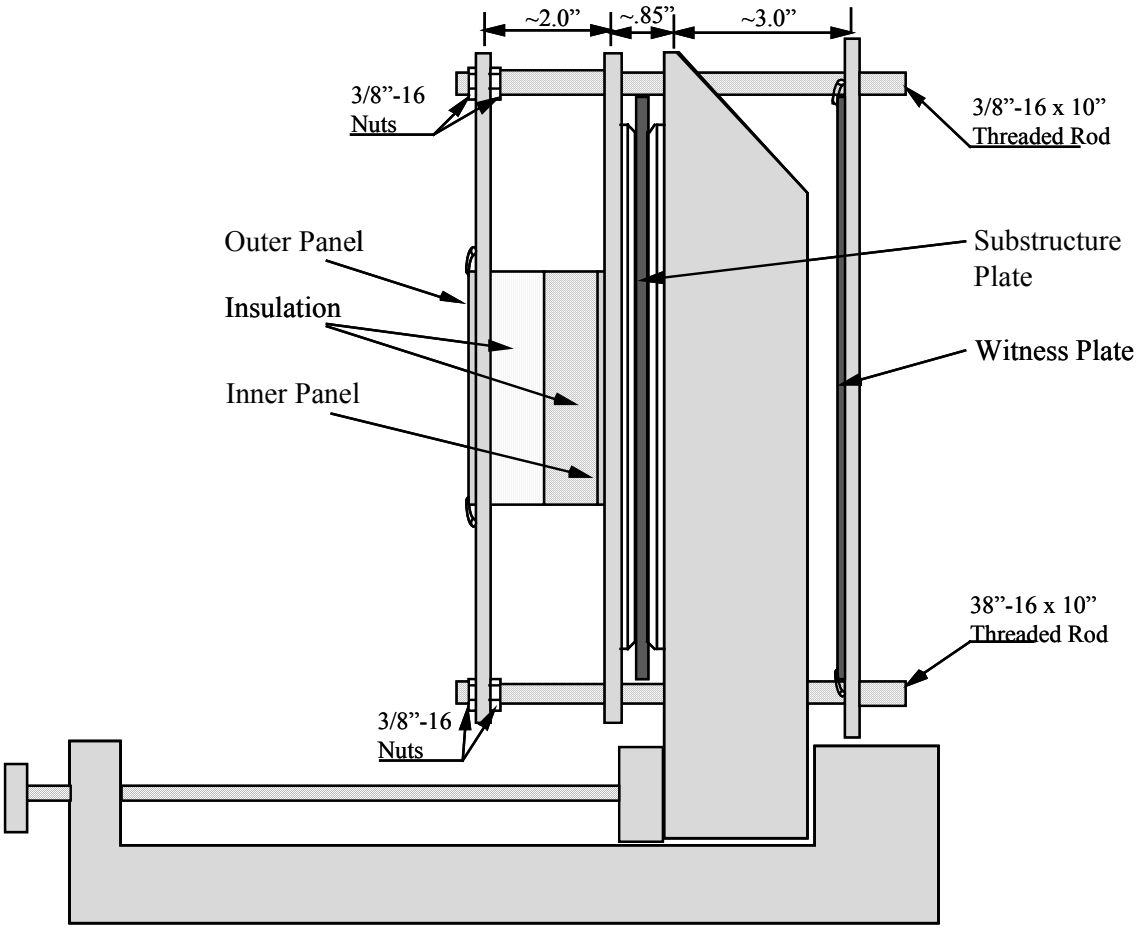

Figure 7: Schematic of hypervelocity impact test specimen holder with metallic TPS elements installed

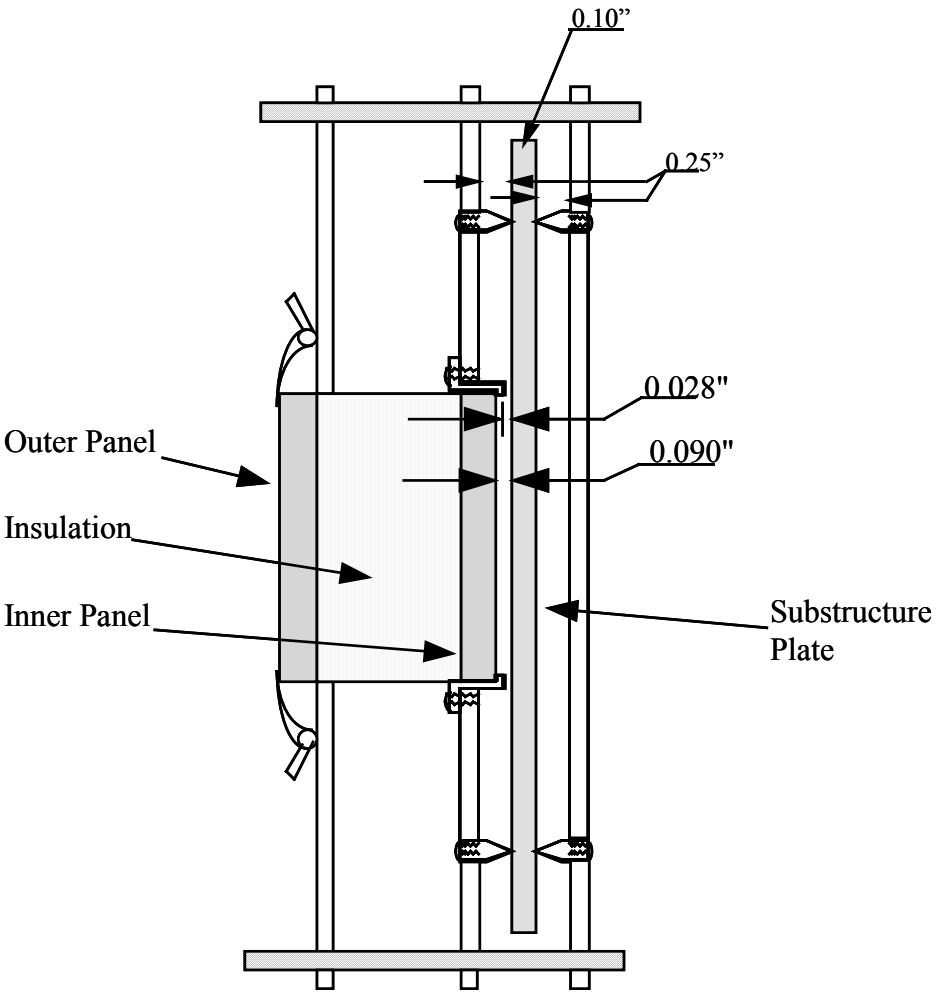

Figure 8: Detail of positioning and support of substructure plate.

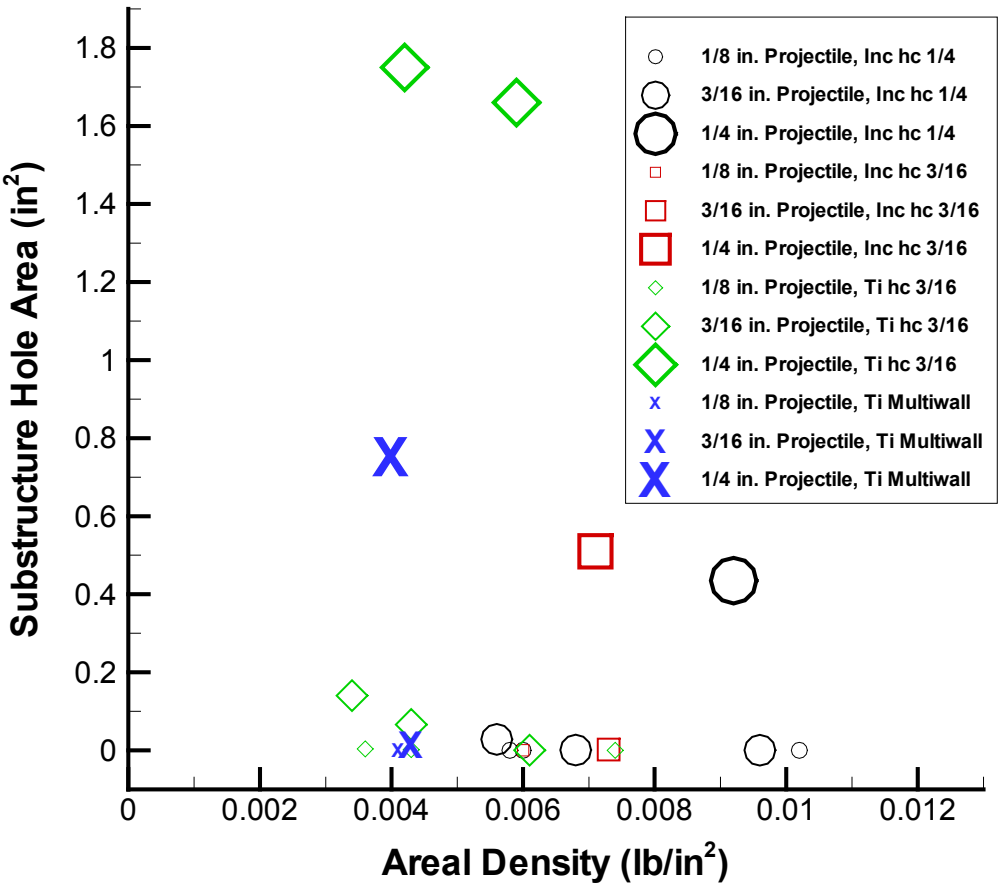

Figure 9: TPS Areal Density vs. Substructure Hole Area for four configurations of TPS tested with three projectile sizes.

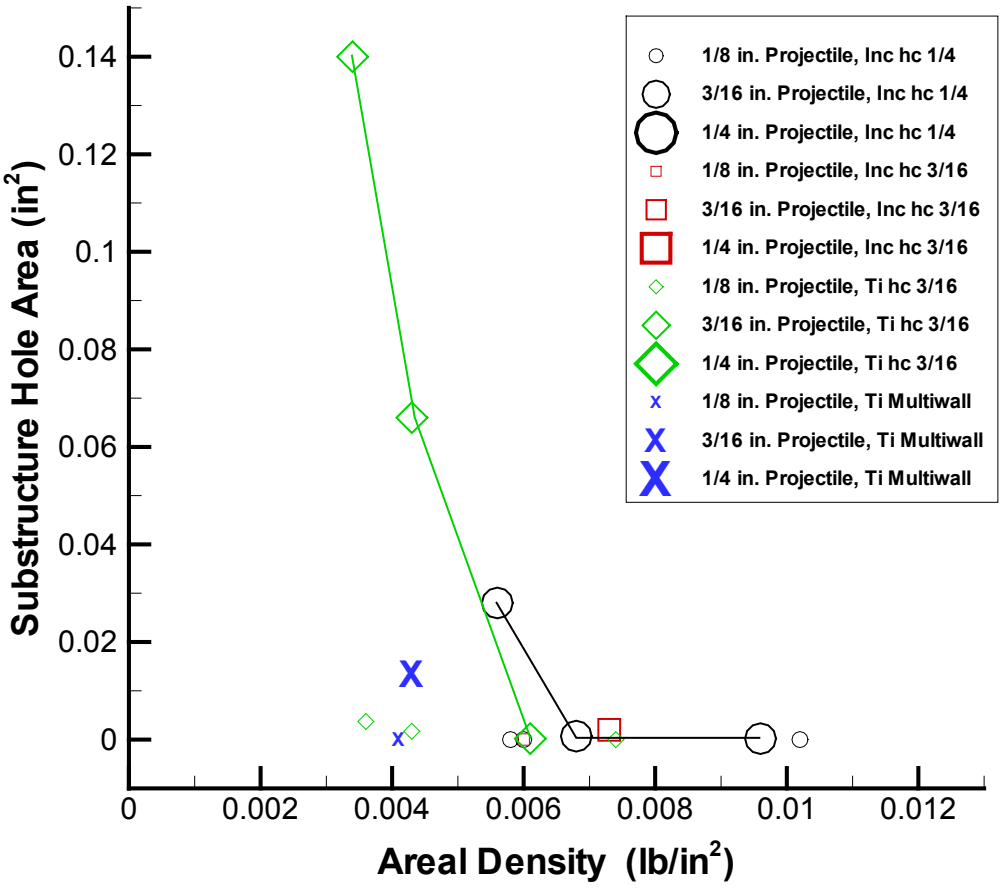

Figure 10: TPS Areal Density vs. Substructure Hole Area focusing on results with 3/16 in. projectiles.

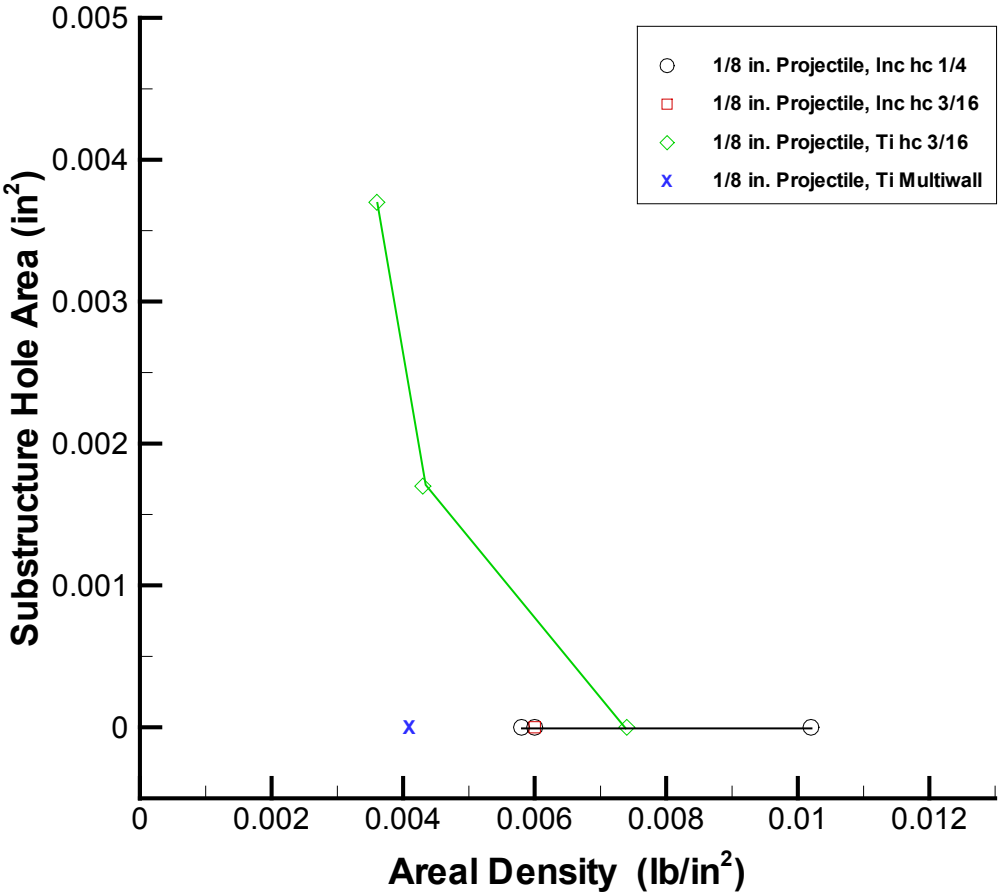

Figure 11: TPS Areal Density vs. Substructure Hole Area for tests with 1/8 in. projectile.

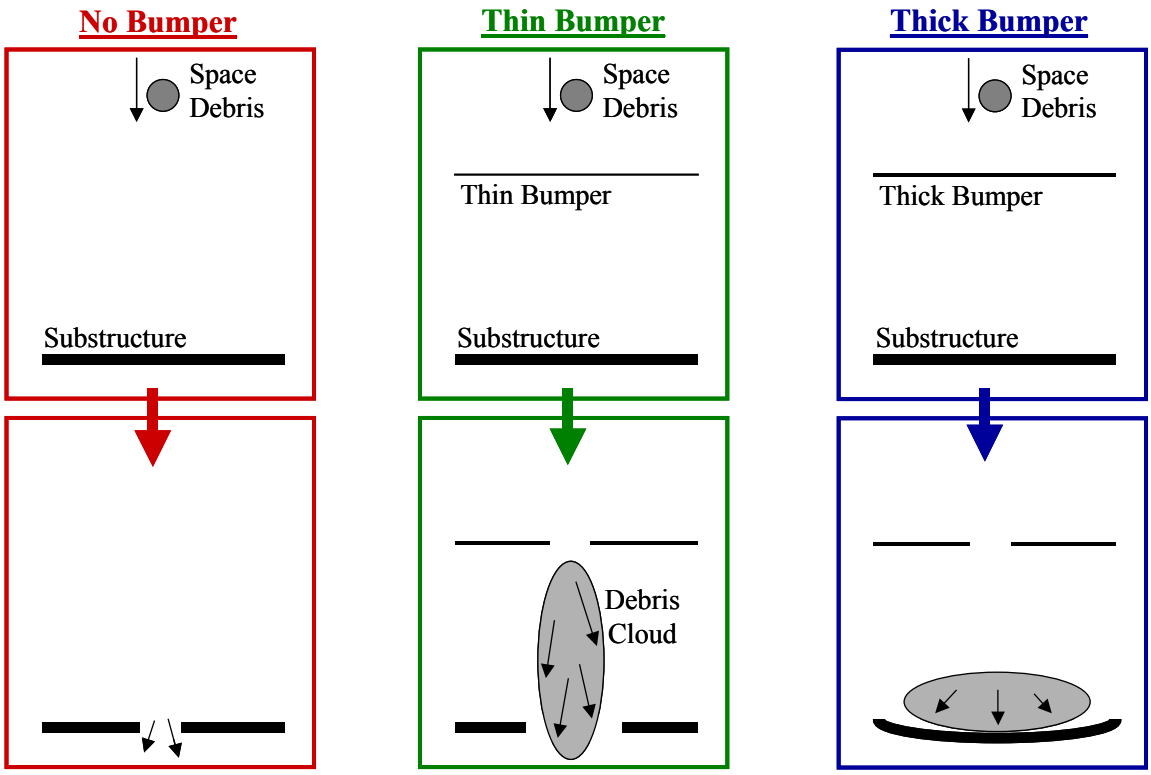

Figure 12: Schematic representation of impact with three different structures. "No Bumper" consists of substructure only, "Thin Bumper" makes use of a ineffective bumper, and "Thick Bumper" makes use of a effective bumper.

Appendix A: Pictures of Hypervelocity Impact Specimens

0.0025 in. Inconel Honeycomb Sandwich - Front Face

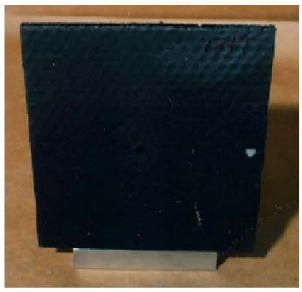

Hole dia. = 0.25 in.

Titanium Foil Front Face

3 holes
1 = 0.7 in. x 0.8 in.
2 = 1.1 in. x 0.4 in.
3 = 6.0 in. x 2.1 in.

Aluminum Substructure Front Face

Debris Spray area = 3.5 in. dia.

0.0025 in. Inconel Honeycomb Sandwich - Back Face

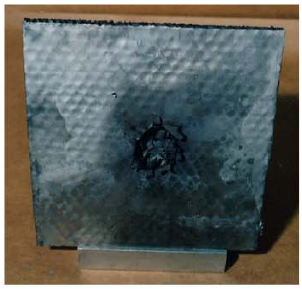

Hole size = 1.2 in. x 1.2 in.

Aluminum Substructure Back Face

4 Holes
1 = 0.1 in. dia.
2 = 0.15 in. x 0.3 in
3 = 0.08 in. dia.
4 = 0.05 in. dia.

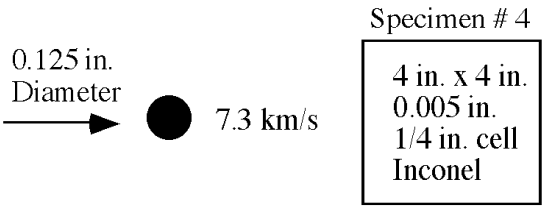

0.005 in. 1/4 in. cell Inconel Honeycomb Sandwich - Front Face

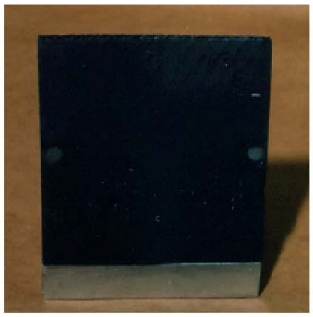

Hole dia. = 0.2 in.

Titanium Foil Front Face

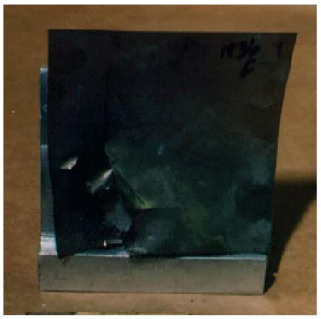

2 Holes
1 = 1.9 in. x 3.3 in.
2 = 0.7 in. x 1.0 in.

Aluminum Substructure

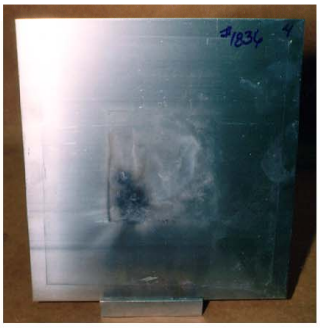

Debris spray area = 2.5 in. dia.

0.005 in. 1/4 in. cell Inconel Honeycomb Sandwich - Front Face

Hole size = 1.0 in. x 0.9 in.

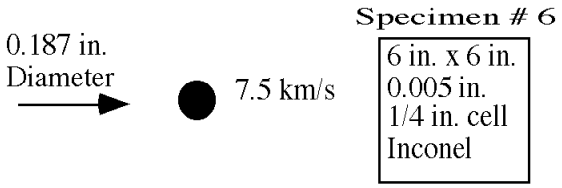

0.005 in. 1/4 in. cell
Inconel Honeycomb
Sandwich - Front Face

Hole size = 0.3 in. x 0.2 in.

Titanium Foil
Front Face

1 piece missing
cannot approximate size

Aluminum Substructure
Front Face

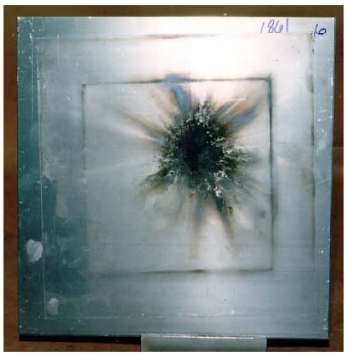

Debris spray area = 2.5 in. dia.
with 1 pin hole

0.005 in. 1/4 in. cell
Inconel Honeycomb
Sandwich - Back Face

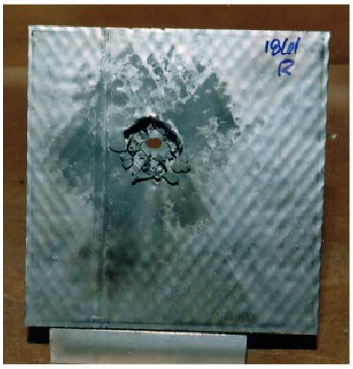

Hole size = 1.2 in. x 1.4 in.

0.01 in. Inconel Honeycomb Sandwich - Front Face

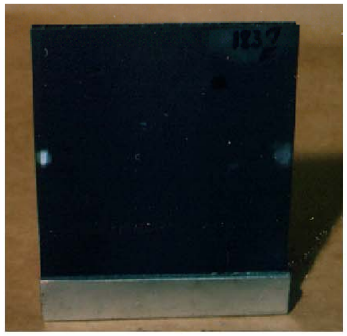

Hole dia. = 0.2 in.

Titanium Foil Front Face

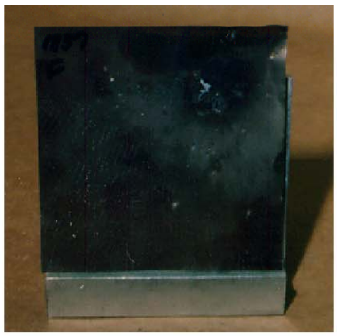

2 holes
1 = 0.35 in. x 0.5 in.
2 = 0.8 in. x 0.15 in.

Aluminum Substructure Front Face

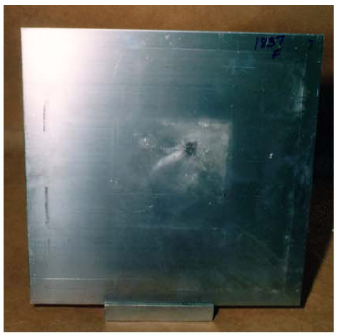

Debris spray area = 1.0 in.

0.01 in. Inconel Honeycomb Sandwich - Back Face

Hole size = 1.0 in. x 0.9 in.

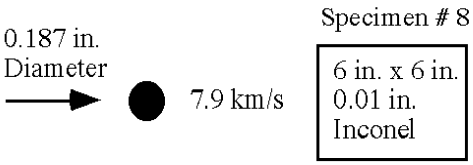

0.01 Inconel Honeycomb Sandwich - Front Face

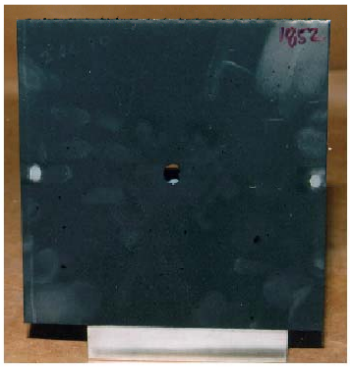

Hole dia. = 0.35 in.

Titanium Foil Front Face

Hole size = 2.0 in. x 2.2 in.

Aluminum Substructure Front Face

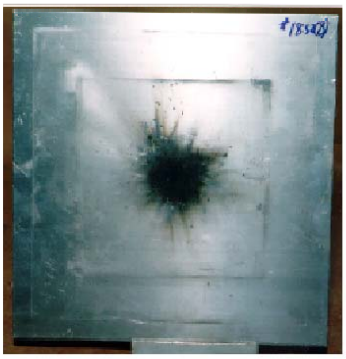

Debris spray area = 2.5 in. dia.

0.01 Inconel Honeycomb Sandwich - Back Face

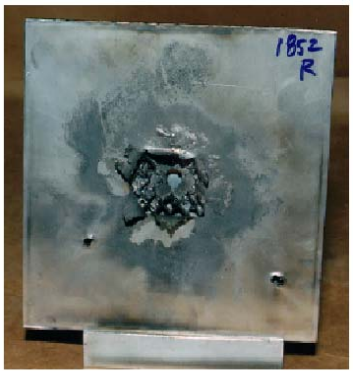

Hole size = 1.7 in. x 1.5 in.

Aluminum Substructure Back Face

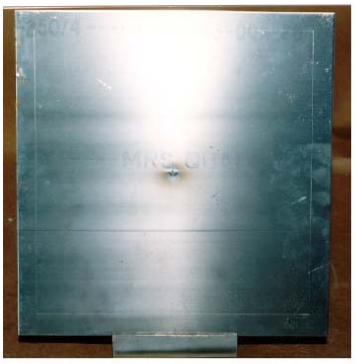

Very small pin hole

0.01 in. Inconel Honeycomb Sandwich - Front Face

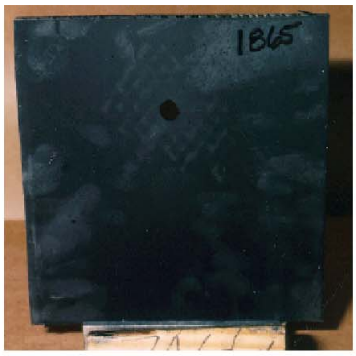

Hole dia. = 0.45 in.

Titanium Foil Front Face

2 Holes
1 = 4.0 in. x 3.1 in.
2 = 0.6 in. x 0.2 in.

Aluminum Substructure Front Face

Hole size = 1.0 in. x 0.8 in.

0.01 in. Inconel Honeycomb Sandwich - Back Face

Hole size = 0.15 in. x 1.3 in.

Aluminum Substructure Back Face

Specimen # 10

0.125 in.
Diameter

7.3 km/s

4 in. x 4 in.
0.005 in.
3/16" cell
Inconel
Oxidized

0.005 in. 3/16" cell Oxidized
Inconel Honeycomb
Sandwich - Front Face

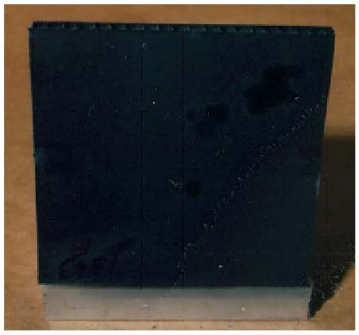

Hole dia. = 0.2 in.

Titanium Foil
Front Face

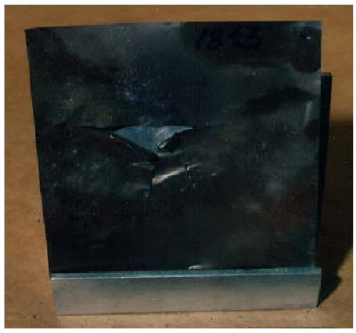

Hole size = 3.5 in. x 1.5 in.

Aluminum Substructure
Front Face

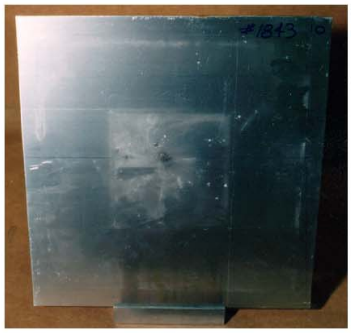

Debris spray area = 2.0 in. dia.

0.005 in. 3/16" cell Oxidized
Inconel Honeycomb
Sandwich - Front Face

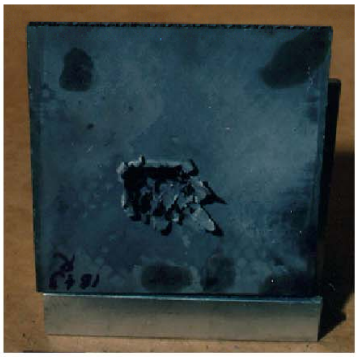

Hole size = 1.1 in. x 0.8 in.

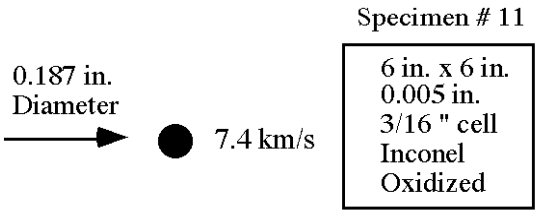

0.005 in. 3/16" cell
Oxidized Inconel Honeycomb
Sandwich - Front Face

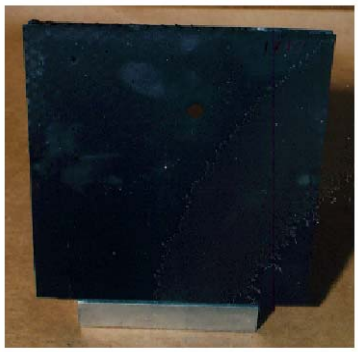

Hole dia. = 0.3 in.

Titanium Foil
Front Face

1 piccc missing
approx. hole = 2.5 in. x 1.9 in.

Aluminum Substructure
Front Face

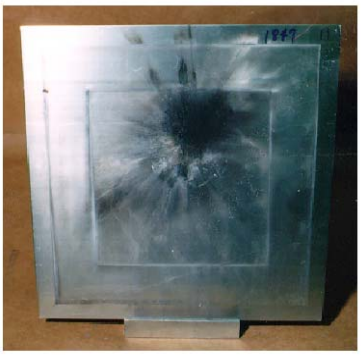

Hole dia. = 0.05 in.

0.005 in. 3/16" cell
Oxidized Inconel Honeycomb
Sandwich - Back Face

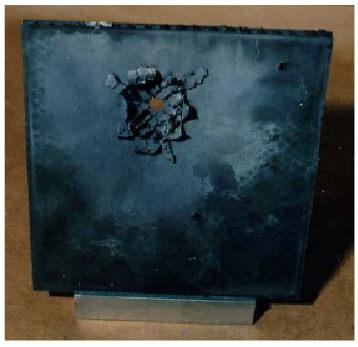

Hole size = 1.4 in. x 1.5 in.

Aluminum Substructure
Back Face

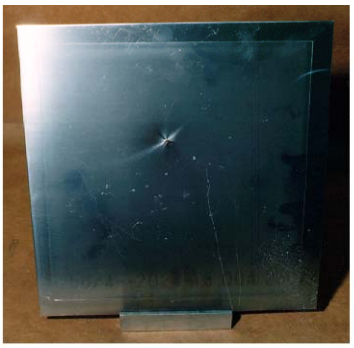

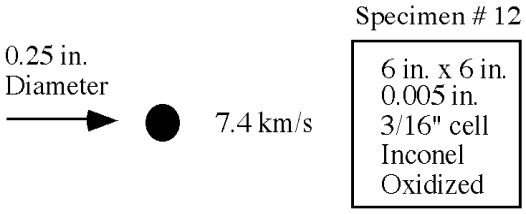

0.005 in. 3/16" cell
Oxidized Inconel Honeycomb
Sandwich - Front Face

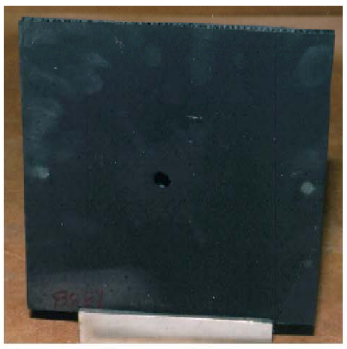

IHole dia. = 0.3 in.

Titanium Foil
Front Face

IHole dia. - 2.5 in.

Aluminum Substructure
Front Face

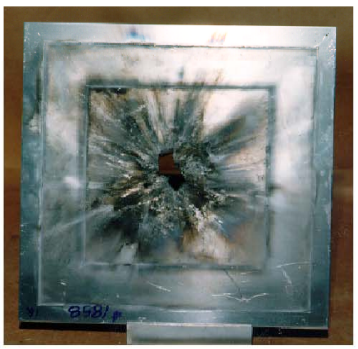

IHole size = 1.5 in. x 1.4 in.

0.005 in. 3/16" cell
Oxidized Inconel Honeycomb
Sandwich - Back Face

Hole size = 1.6 in. x 1.4 in.

Aluminum Substructure
Back Face

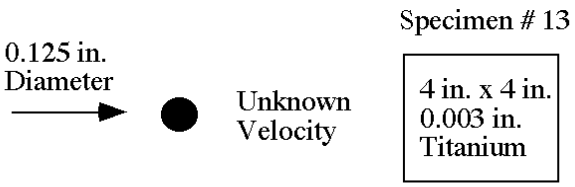

0.003 in. Titanium Honeycomb Sandwich - Front Face

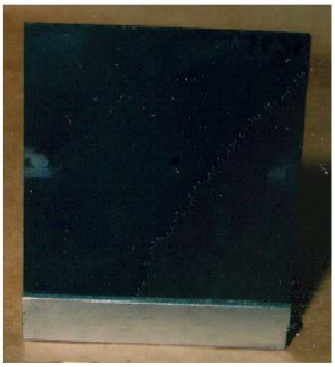

Hole dia. = 0.15 in.

Titanium Foil Front Face

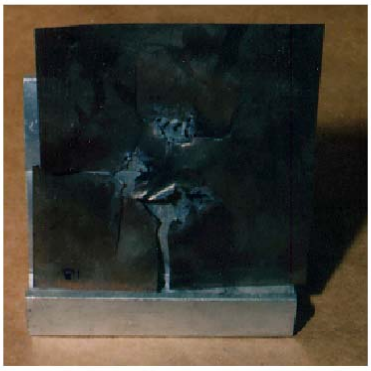

3 Holes
1 = 0.8 in. x 0.5 in.
2 = 0.4 in. x 0.4 in.
3 = 0.5 in. x 0.3 in.

Aluminum Substructure Front Face

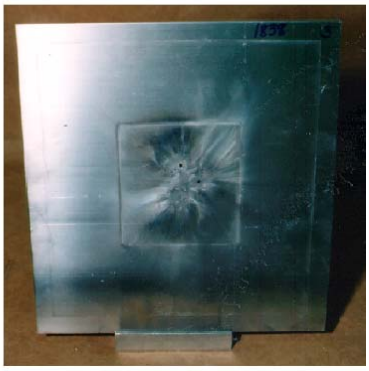

3 Holes at 0.1 in. dia. each

0.003 in. Titanium Honeycomb Sandwich - Back Face

Hole size = 0.8 in. x 0.7 in.

Aluminum Substructure Back Face

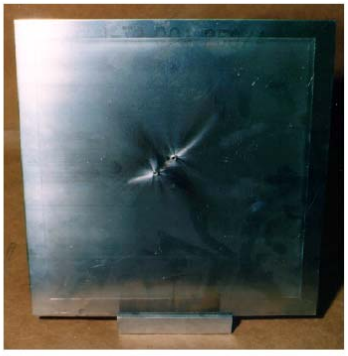

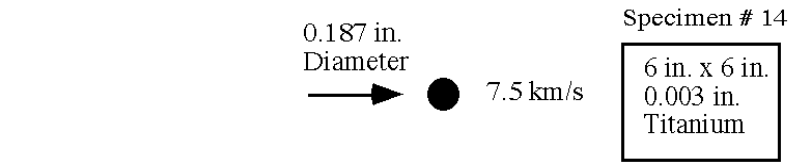

0.003 in. Titanium Honeycomb Sandwich - Front Face

Hole dia. = 0.2 in.

Titanium Foil Front Face

Hole size = 3.2 in. x 2.9 in.

Aluminum Substructure Front Face

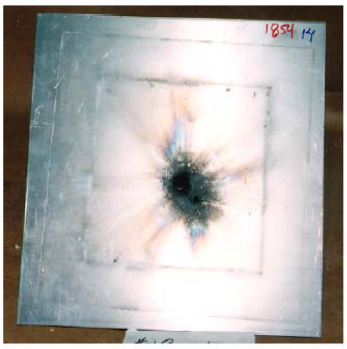

2 Holes
1 = 0.45 in. dia.
2 = 0.1 in. dia.

0.003 in. Titanium Honeycomb Sandwich - Back Face

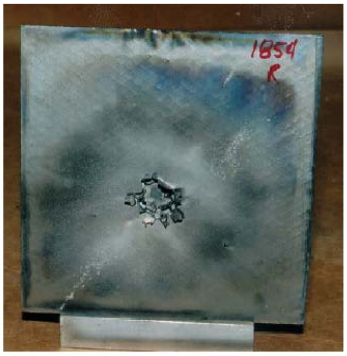

Hole size = 0.9 in. x 0.8 in.

Aluminum Substructure Back Face

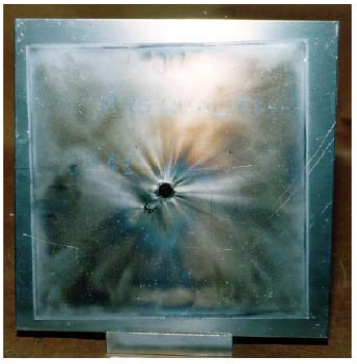

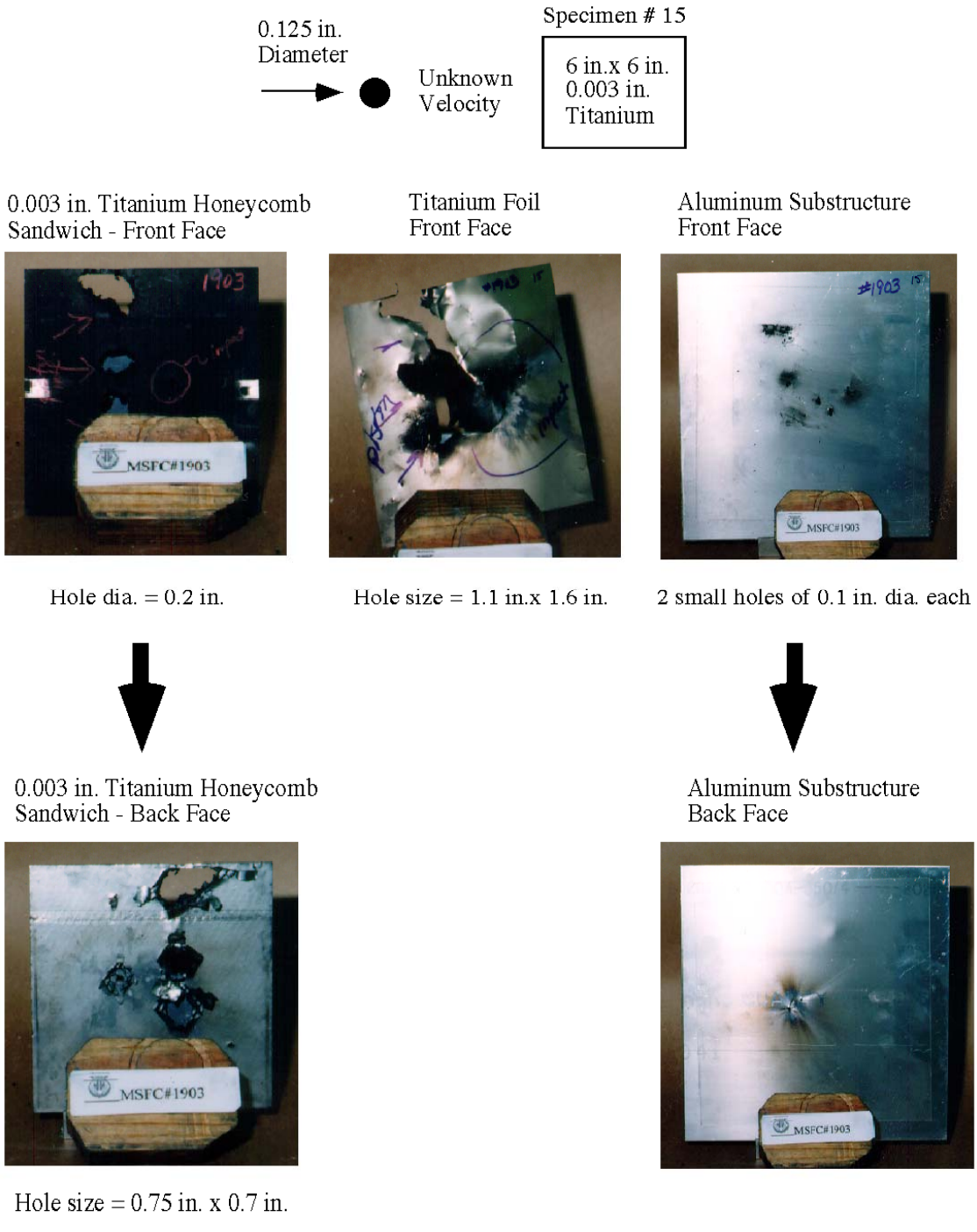
0.125 in.
Diameter
Unknown
Velocity
Specimen # 15
6 in.x 6 in.
0.003 in.
Titanium
0.003 in. Titanium Honeycomb
Sandwich - Front Face
Titanium Foil
Front Face
Aluminum Substructure
Front Face
MSFC#1903
Hole dia. = 0.2 in.
Hole size = 1.1 in.x 1.6 in.
2 small holes of 0.1 in. dia. each
0.003 in. Titanium Honeycomb
Sandwich - Back Face
Aluminum Substructure
Back Face
Hole size = 0.75 in. x 0.7 in.

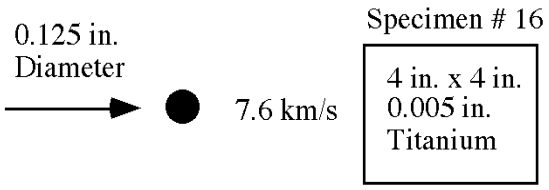

0.005 in. Titanium Honeycomb Sandwich - Front Face

Hole dia. = 0.15 in.

Titanium Foil Front Face

2 small holes
1 = 0.1 in. dia.
2 = 0.25 in. x 0.1 in.

Aluminum Substructure Front Face

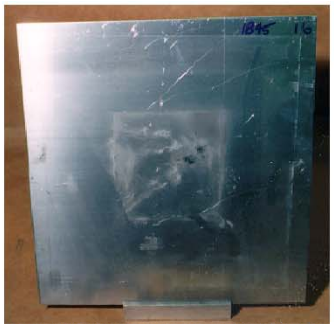

2 small holes 0.05 in. dia. each

0.005 in. Titanium Honeycomb Sandwich - Back Face

Hole size = 1.1 in. x 1.8 in.

Aluminum Substructure Back Face

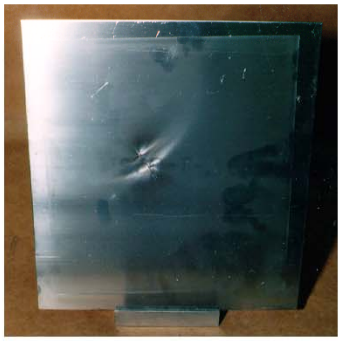

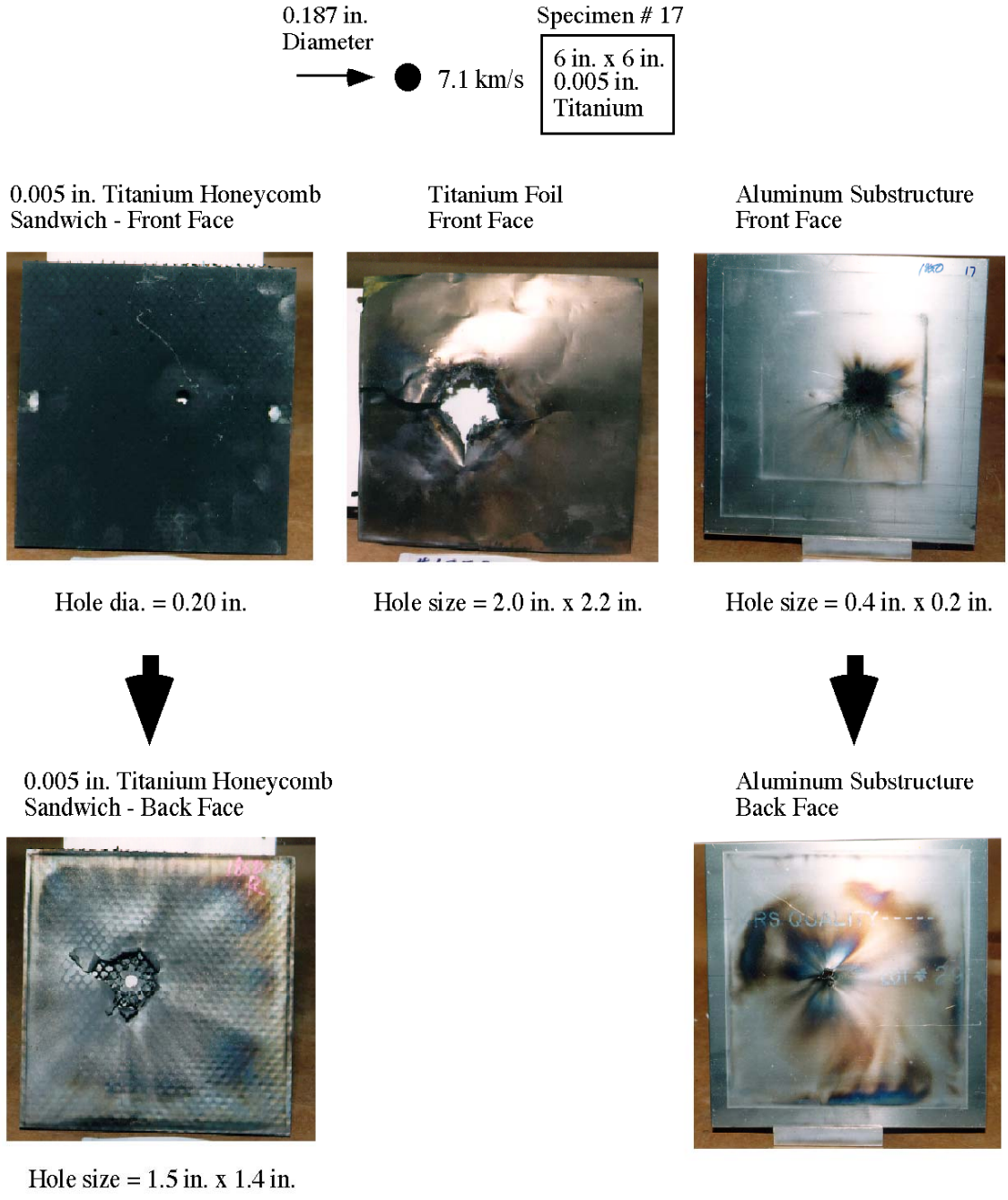
0.187 in.
Diameter
7.1 km/s
Specimen # 17
6 in. x 6 in.
0.005 in.
Titanium
0.005 in. Titanium Honeycomb
Sandwich - Front Face
Titanium Foil
Front Face
Aluminum Substructure
Front Face
Hole dia. = 0.20 in.
Hole size = 2.0 in. x 2.2 in.
Hole size = 0.4 in. x 0.2 in.
0.005 in. Titanium Honeycomb
Sandwich - Back Face
Aluminum Substructure
Back Face
Hole size = 1.5 in. x 1.4 in.

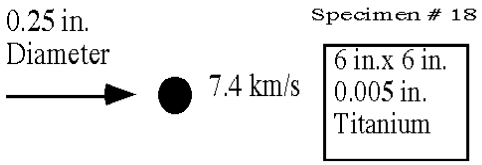

0.005 in. Titanium Honeycomb Sandwich - Front Face

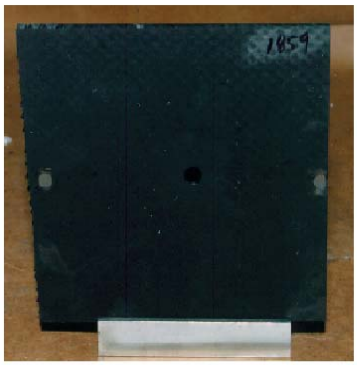

Hole dia. = 0.3 in.

Titanium Foil Front Face

Hole size = 3.0 in. x 4.2 in.

Aluminum Substructure Front Face

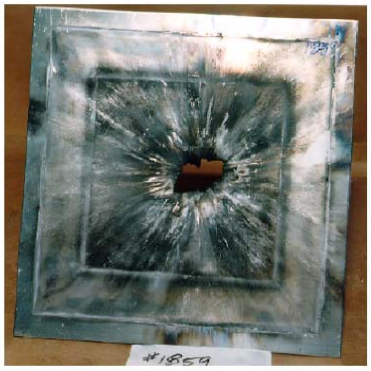

Hole size = 1.8 in. x 1.5 in.

0.005 in. Titanium Honeycomb Sandwich - Back Face

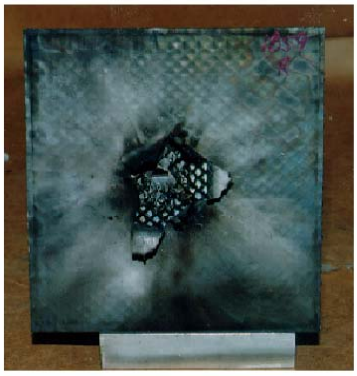

Hole size = 2.0 in. x 1.8 in.

Aluminum Substructure Back Face

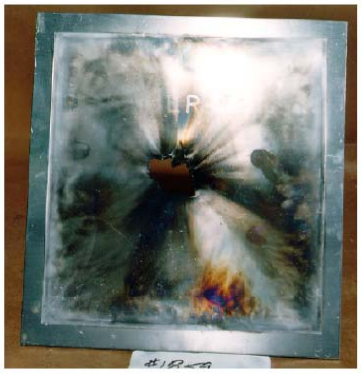

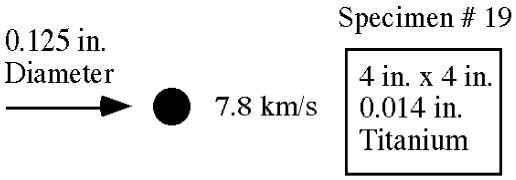

0.014 in. Titanium Honeycomb Sandwich - Front Face

Hole dia. = 0.2 in.

Titanium Foil Front Face

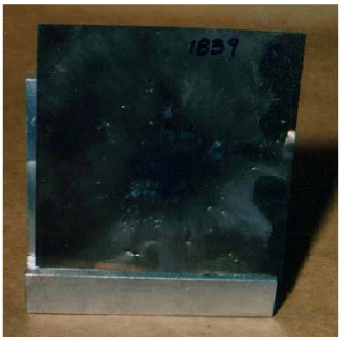

Debris spray area = 3.5 in.

Aluminum Substructure Front Face

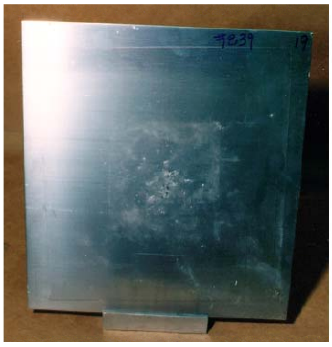

Debris spray area = 2.5 in.

0.014 in. Titanium Honeycomb Sandwich - Back Face

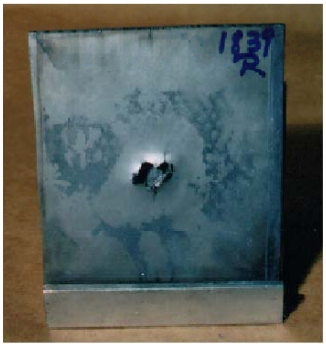

Hole size = 0.8 in. x 0.5 in.

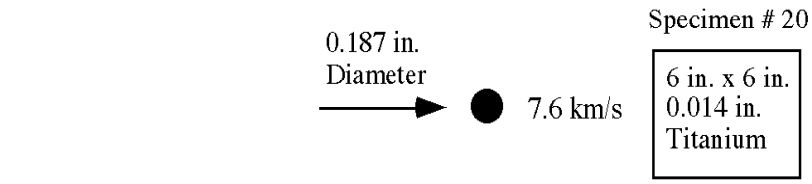

0.014 in. Titanium Honeycomb Sandwich - Front Face

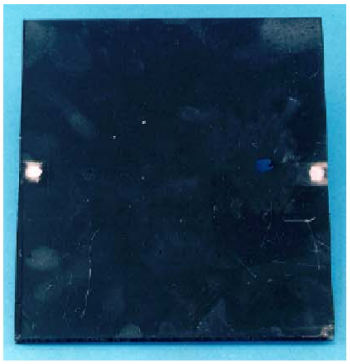

Hole size = 0.1 in. x 0.25 in.

Titanium Foil Front Face

Hole size = 2.3 in. x 2.4 in.

Aluminum Substructure Front Face

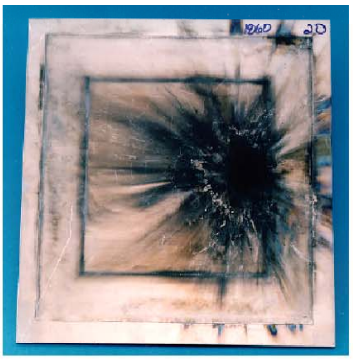

Debris spray area = 4.0 in. dia. with a small pin hole

0.014 in. Titanium Honeycomb Sandwich - Back Face

Hole size = 1.0 in. x 1.2 in.

Aluminum Substructure Back Face

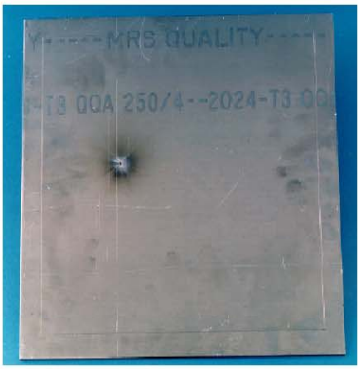

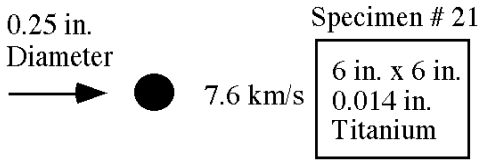

0.014 in. Titanium Honeycomb Sandwich - Front Face

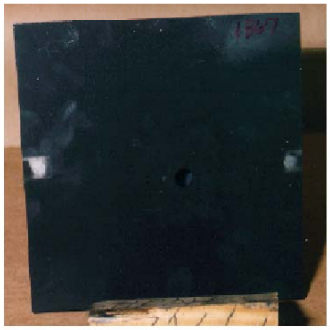

Hole dia. = 0.35 in.

Titanium Foil Front Face

Hole size = 2.5 in. x 3.2 in.

Aluminum Substructure Front Face

Hole size = 1.4 in. x 1.0 in.

0.014 in. Titanium Honeycomb Sandwich - Back Face

Hole size = 0.9 in. x 0.8 in.

Aluminum Substructure Back Face

Specimen # 25

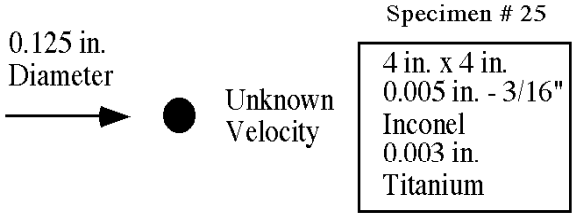

0.005 in. 3/16 in. cell Inconel Honeycomb Sandwich Front Face

Hole dia. = 0.2 in.

0.003 in. Titanium Honeycomb Sandwich - Front Face

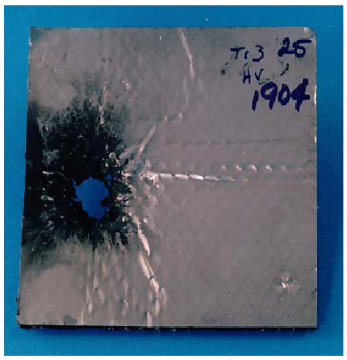

Hole size = 1.0 in. x 0.5 in.

Aluminum Substructure Front Face

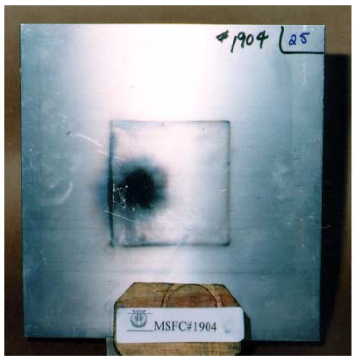

Debris spray area = 1.5 in. dia.

0.005 in. 3/16 in. cell Inconel Honeycomb Sandwich Back Face

Hole size = 1.0 in. x 0.75 in.

0.003 in. Titanium Honeycomb Sandwich - Back Face

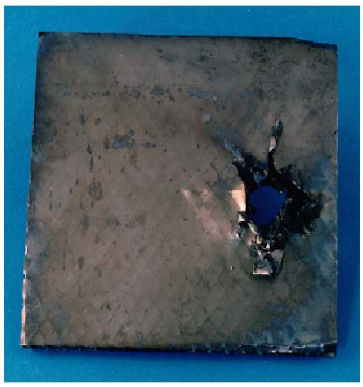

Hole size = 1.6 in. x 1.2 in.

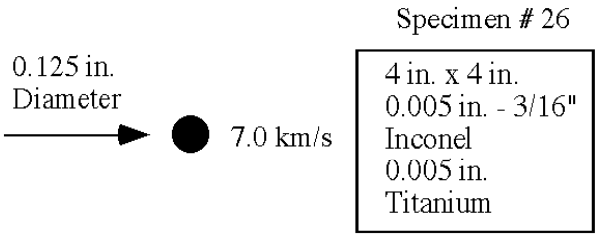

0.005 in. 3/16 in. cell Inconel Honeycomb Sandwich Front Face

Hole dia. = 0.15 in.

0.005 in. Titanium Honeycomb Sandwich - Front Face

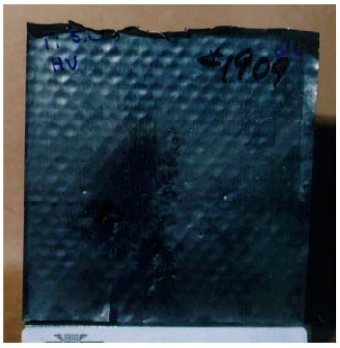

Hole size = 0.4 in.x 0.5 in.

Aluminum Substructure Front Face

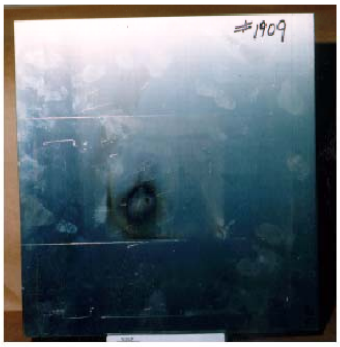

Debris spray area = 1.0 in. dia.

0.005 in. 3/16 in. cell Inconel Honeycomb Sandwich Back Face

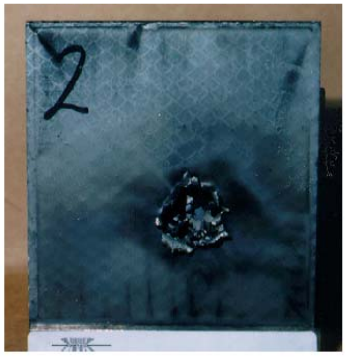

Hole size = 0.2 in.x 0.9 in.

0.005 in. Titanium Honeycomb Sandwich - Back Face

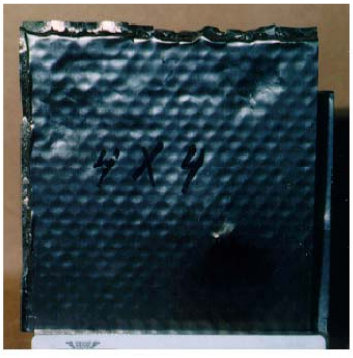

Hole size = 0.3 in. crack

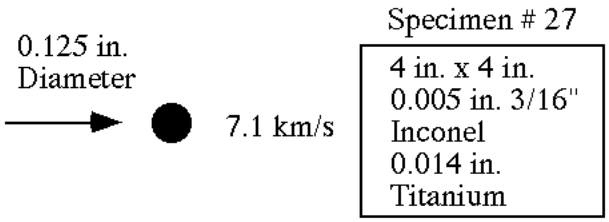

0.005 in. 3/16 in. cell Inconel Honeycomb Sandwich Front Face

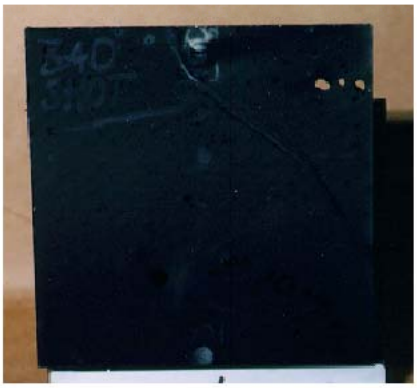

Hole dia. = 0.2 in.

0.005 in. 3/16 in. cell Inconel Honeycomb Sandwich Back Face

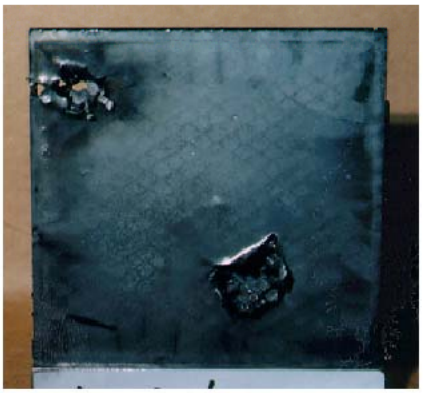

Hole size = 1.1 in. x 0.9 in.

0.014 in. Titanium Honeycomb Sandwich - Front Face

Hole = 0.5 in. dia.
with 2.0 in. debris spray

0.014 in. Titanium Honeycomb Sandwich - Back Face

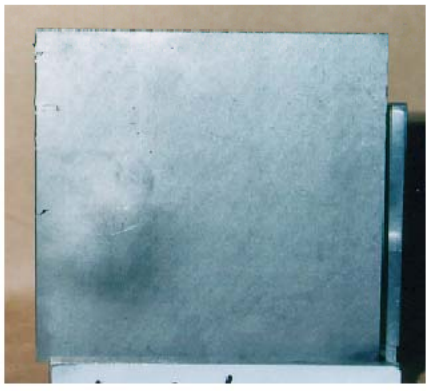

No damage

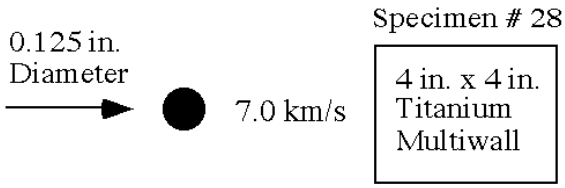

Titanium Multiwall
Front Face

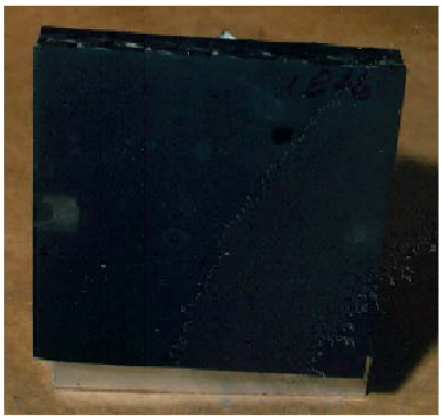

Hole dia. = 0.2 in.

Aluminum Substructure

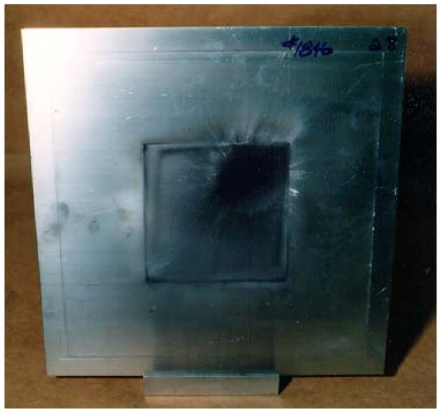

Debris spray area = 4.0 in.

Titanium Multiwall
Back Face

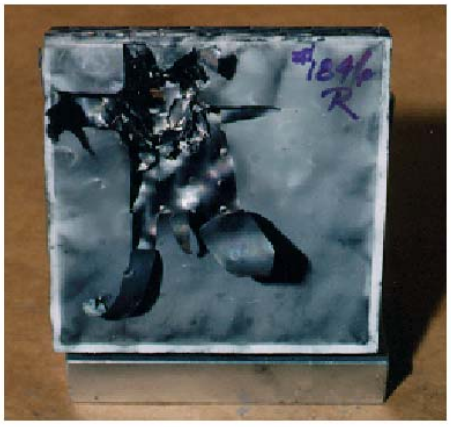

Hole size
inside = 1.0 in. dia.
outside = 2.5 in. x 2.5 in.

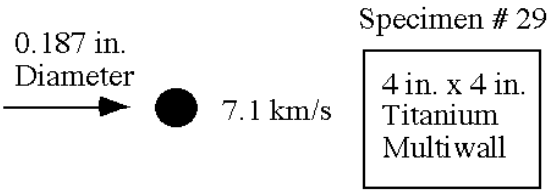

Titanium Multiwall
Front Face

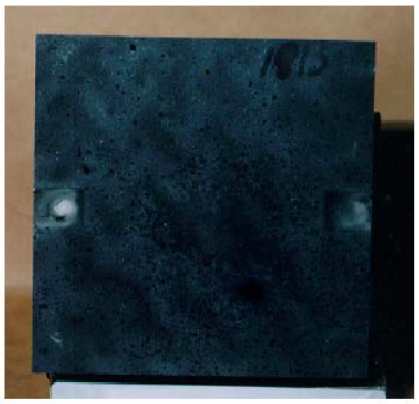

Hole dia. = 0.25 in.

Titanium Multiwall
Back Face

2 Holes
1 = 1.1 in. dia.
2 = 2.5 in. x 2.4 in.

Aluminum Substructure
Front Face

Debris spray area = 6.0 in. dia.
with a small pin hole

Aluminum Substructure
Back Face

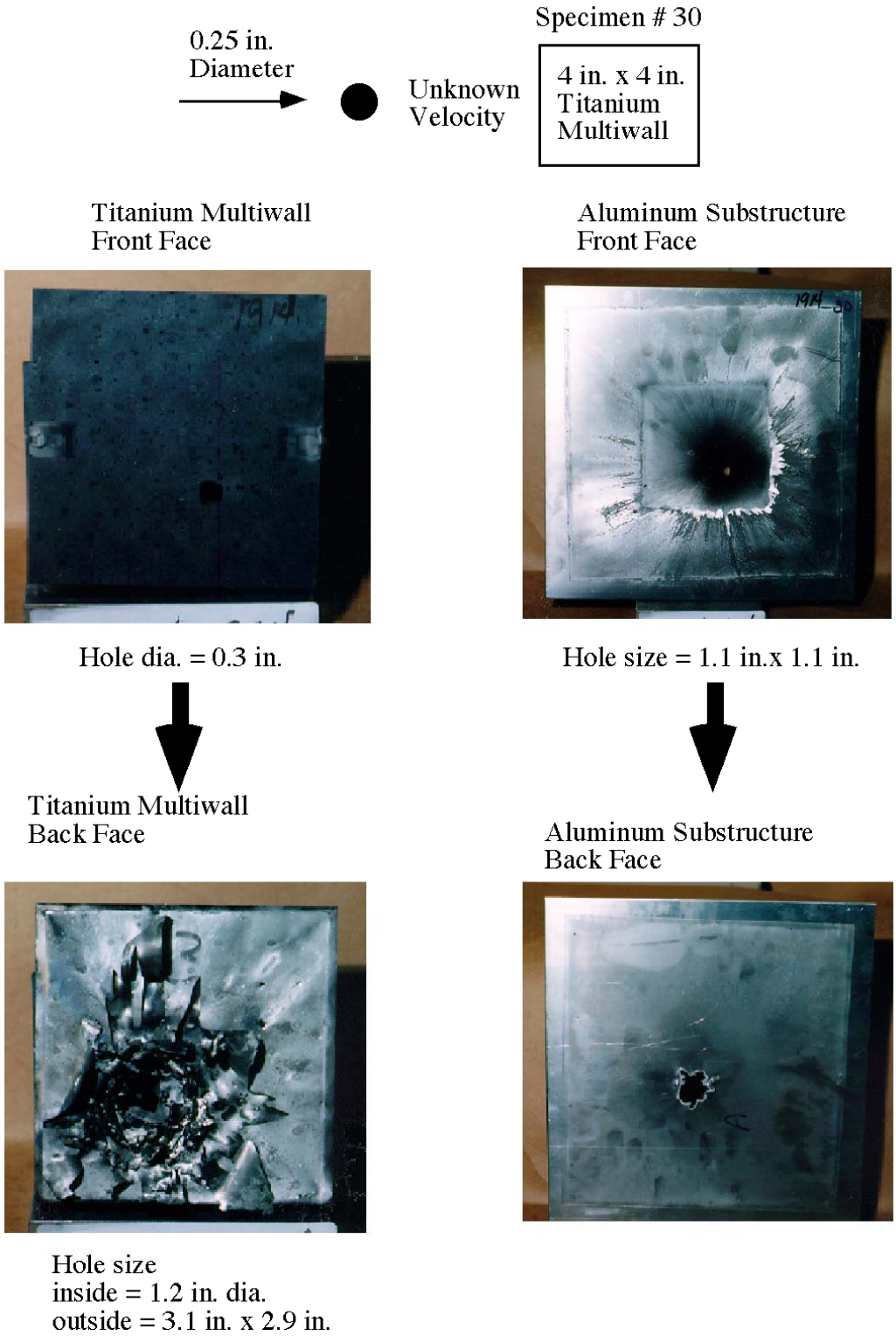
Specimen # 30
0.25 in.
Diameter
Unknown
Velocity
4 in. x 4 in.
Titanium
Multiwall
Titanium Multiwall
Front Face
Aluminum Substructure
Front Face
Hole dia. = 0.3 in.
Hole size = 1.1 in.x 1.1 in.
Titanium Multiwall
Back Face
Aluminum Substructure
Back Face
Hole size
inside = 1.2 in. dia.
outside = 3.1 in. x 2.9 in.

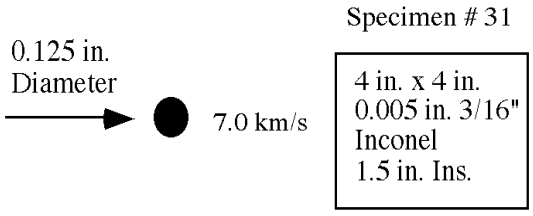

0.005 in. 3/16 in. cell Inconel
Honeycomb Sandwich
Front Face

Hole dia. = 0.15 in.

Titanium Foil
Front Face

Hole size = 1.7 in. x 1.4 in.

Aluminum Substructure
Front Face

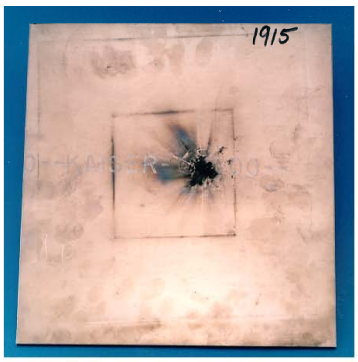

Debris spray area = 2.0 in. dia.

0.005 in. 3/16 in. cell Inconel
Honeycomb Sandwich
Back Face

Hole size = 1.0 in. x 0.8 in.

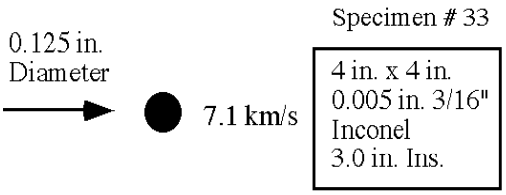

0.005 in. 3/16 in. cell Inconel Honeycomb Sandwich Front Face

Hole dia. = 0.2 in.

Titanium Foil Front Face

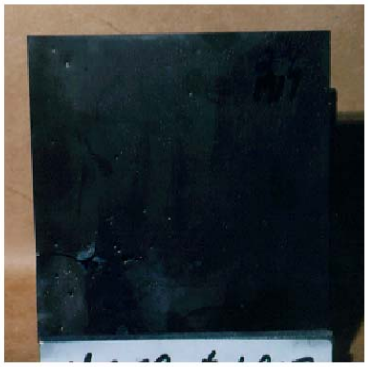

Hole size = 0.2 in. x 0.15 in.

Aluminum Substructure Front Face

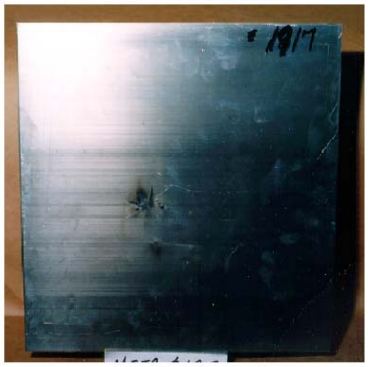

Hole dia. = 0.1 in.

0.005 in. 3/16 in. cell Inconel Honeycomb Sandwich Back Face

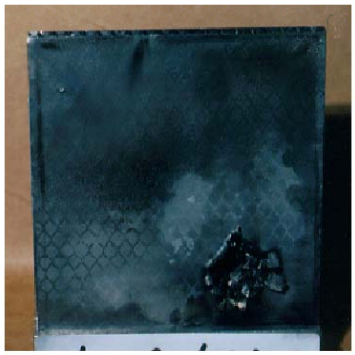

Hole size = 0.9 in. x 0.85 in.

Aluminum Substructure Back Face

REPORT DOCUMENTATION PAGE

Form Approved
OMB No. 0704-0188

1. AGENCY USE ONLY (*Leave blank*)	2. REPORT DATE	3. REPORT TYPE AND DATES COVERED
	August 2003	Technical Memorandum

4. TITLE AND SUBTITLE
Hypervelocity Impact Test Results for a Metallic Thermal Protection System

5. FUNDING NUMBERS
721-21-87-07

6. AUTHOR(S)
Katherine L. Karr, Carl C. Poteet, and Max L. Blosser

7. PERFORMING ORGANIZATION NAME(S) AND ADDRESS(ES)
NASA Langley Research Center
Hampton, VA 23681-2199

8. PERFORMING ORGANIZATION REPORT NUMBER
L-18192

9. SPONSORING/MONITORING AGENCY NAME(S) AND ADDRESS(ES)
National Aeronautics and Space Administration
Washington, DC 20546-0001

10. SPONSORING/MONITORING AGENCY REPORT NUMBER
NASA/TM-2003-212440

11. SUPPLEMENTARY NOTES
Karr: The George Washington University, JIAFS; Poteet: Langley Research Center, Hampton, VA; Blosser: Langley Research Center, Hampton, VA

12a. DISTRIBUTION/AVAILABILITY STATEMENT
Unclassified-Unlimited
Subject Category 15 Distribution: Standard
Availability: NASA CASI (301) 621-0390

12b. DISTRIBUTION CODE

13. ABSTRACT *(Maximum 200 words)*
Hypervelocity impact tests have been performed on specimens representing metallic thermal protection systems (TPS) developed at NASA Langley Research Center for use on next-generation reusable launch vehicles (RLV). The majority of the specimens tested consists of a foil gauge exterior honeycomb panel, composed of either Inconel 617 or Ti-6Al-4V, backed with 2.0 in. of fibrous insulation and a final Ti-6Al-4V foil layer. Other tested specimens include titanium multi-wall sandwich coupons as well as TPS using a second honeycomb sandwich in place of the foil backing. Hypervelocity impact tests were performed at the NASA Marshall Space Flight Center Orbital Debris Simulation Facility. An improved test fixture was designed and fabricated to hold specimens firmly in place during impact. Projectile diameter, honeycomb sandwich material, honeycomb sandwich facesheet thickness, and honeycomb core cell size were examined to determine the influence of TPS configuration on the level of protection provided to the substructure (crew, cabin, fuel tank, etc.) against micrometeoroid or orbit debris impacts. Pictures and descriptions of the damage to each specimen are included.

14. SUBJECT TERMS
hypervelocity impact; orbital debris; metallic thermal protection system; hypervelocity impact simulation, hypervelocity impact simulation

15. NUMBER OF PAGES
79

16. PRICE CODE

17. SECURITY CLASSIFICATION OF REPORT	18. SECURITY CLASSIFICATION OF THIS PAGE	19. SECURITY CLASSIFICATION OF ABSTRACT	20. LIMITATION OF ABSTRACT
Unclassified	Unclassified	Unclassified	UL